EVALUATION OF FILTERING METHODS FOR HYDROGRAPH SEPARATION IN SMALL AGRICULTURAL WATERSHEDS IN QUÉBEC, CANADA

F. Umuhire, F. Anctil, A. R. Michaud, J. Desjardins

HIGHLIGHTS

- Agricultural hydrology is complex due to the management of surface and subsurface flow to increase productivity.
- This study provides an interpretation of hydrological functioning, using a geochemical tracer (electrical conductivity) as a reference method, for hydrograph separation and evaluation of filtering methods.
- Filtering method efficiency must be interpreted according to season, year, watershed relief, and management practices.
- Routine application of basic filtering concepts is not sufficient to address the heterogeneity of hydrological processes in agricultural watersheds.

ABSTRACT. *Streamflow hydrographs summarize the behavior of watersheds. Their separation into quick and slow components requires hydrological knowledge of the specific drainage area. To better understand the hydrological response of 14 small agricultural watersheds in Québec, Canada, covering different physiographic attributes ranging from lowlands to hilly and steep landscapes, streamflow electrical conductivity was used as a geochemical tracer. These agricultural watersheds have undergone significant management practices, including artificial drainage. The objective of this research was to evaluate the performance of existing automated filter methods for hydrograph separation (BFLOW, UKIH, PART, FIXED, SLIDE, LOCMIN, and Eckhardt). The geochemical method was used as a reference for comparison with the filter methods. Comparison of the slow flow estimates from non-calibrated filters, using a MANOVA model, showed that the filter performance increased under conditions with high contributions of quick runoff to the stream, such as during snowmelt (spring season), during heavy precipitation, and in subwatersheds with landscape conditions more prone to quick runoff. However, filter performance decreased as hydrological processes predisposed more flow to slower pathways, typically in summer and fall, as well as in lowland landscapes generally associated with high rates of tile drainage rather than in hilly and steep relief. Underlying the filter assumptions is the classic concept of a rainfall event with quick runoff as the main source of the drainage area response. Thus, slow flow is associated with a low threshold response. Eckhardt filter simulations were in good agreement with the geochemical method after calibration, based on model statistical measures (R, NSE, and PBIAS). However, larger errors were associated with higher flow values. The slow flow overestimations were more pronounced during periods of extreme events, i.e., spring runoff and heavy precipitation. The linear concept of the Eckhardt filter yields no information on slow flow response behavior that could be useful in capturing its temporal variability. Because the routing of water has been managed to improve agricultural productivity, these hydrological modifications resulted in a more complex slow flow response. The performance of filtering methods is thus affected. Therefore, simplifications of filter assumptions are less likely to provide more effective estimates of slow flow. Furthermore, given the heterogeneity of hydrological processes due to seasonal climatic characteristics, the routine application of basic filter concepts is not sufficient to address the variable nature of the hydrological response. The variability scale of geochemical separation, from regional (agro-climatic) to local (adjacent watersheds), proved that it is always relevant to have adequate separation. However, the validation of filters without a tracer is limited and almost unsuitable for these agricultural watersheds.*

Keywords. *Agricultural watershed, Artificial drainage, Electrical conductivity, Filtering method, Geochemical method, Hydrograph separation, MANOVA, Quick flow, Slow flow, Tile drainage.*

Submitted for review in March 2019 as manuscript number NRES 13434; approved for publication as a Research Article by the Natural Resources & Environmental Systems Community of ASABE in April 2020.

The authors are **Flora Umuhire,** Doctoral Candidate, and **François Anctil,** Professor, Department of Civil and Water Engineering, Université Laval, Québec City, Québec, Canada; **Aubert R. Michaud,** Researcher, and **Jacques Desjardins,** Technician, Institut de Recherche et de Développement en Agroenvironnement (IRDA), Québec City, Québec, Canada. **Corresponding author:** Flora Umuhire, Pavillon Adrien-Pouliot, 1065 Avenue de la Médecine, Québec, QC, Canada G1V 0A6; phone: 418-573-0890; e-mail: flora.umuhire.1@ulaval.ca.

From the 1960s onward, considerable investment in lowland development in the southwestern rural watersheds of Québec Province, Canada, has drastically changed the hydrology of the whole territory. The creation of municipal drains and ditches has allowed the installation of systematic subsurface drainage systems, which have considerably improved the productivity of cropping systems facing short and humid growing seasons.

Typically, where agriculture is intensively practiced, drainage density has reached 1.7 to 2.1 km km^{-2}, which nearly doubles the natural stream network density (Beaulieu, 2001). The artificial drainage of agricultural fields provides additional pathways for the movement of water to the streams, allowing rainfall to move quickly through the landscape (Smith, 2012; Smith and Capel, 2018). The presence of subsurface drainage systems thus affects the hydrological response of watersheds and changes the groundwater flow system. The increase in soil storage capacity has an effect on runoff as soil saturation is delayed due to subsurface drainage, thus increasing stream baseflow (Fraser and Fleming, 2001; Blann et al., 2009). Baseflow, also referred to as slow flow, is a streamflow component that is attributed to groundwater flow and other delayed sources (Hall, 1968; Santhi et al., 2008; Stoelzle et al., 2019). Baseflow is hence referred to as slow flow in this article. Within the subsurface drained watersheds of southwestern Québec, subsurface drainage flow has become the dominant pathway of the hydrological system (Enright and Madramootoo, 2004; Deslandes et al., 2007; Michaud et al., 2009a, 2019; Poirier et al., 2012). The stream slow flow therefore includes groundwater seepage and a variable contribution from subsurface drainage tiles (Schilling and Helmers, 2008; Michaud et al., 2019).

Quantifying the relative contributions of different water sources from a streamflow hydrograph is important for understanding the hydrology and water quality dynamics of a given watershed. The shape of the hydrograph is highly dependent on its physiographic characteristics. The concentration time, i.e., the maximum time required for a drop of water to reach the outlet of the watershed through runoff, partially characterizes the speed and intensity of the watershed's response to a precipitation event. It is influenced by various morphological characteristics of the watershed, such as area, shape, and slope. In addition to these factors, there is also the influence of hydrometeorological parameters, which vary according to altitude (precipitation, temperature, wind, and solar radiation), soil type (infiltration and retention properties, permeability) and land use. Hydrograph separation is considered the first step in the analysis of the water balance at the watershed scale. The basic assumption of hydrograph separation is that streamflow components have different time responses. Thus, the contribution of surface runoff ceases first, while groundwater flow continues after the end of subsurface runoff. During low flows, groundwater provides most or all of the streamflow.

There is a wide variety of hydrograph separation methods. They can be grouped into three categories according to the approach used: conceptual (graphical), filter-based, and experimental.

The conceptual approach is based on the assumption that a typical event hydrograph is the result of the superposition of two flows: a slow flow that essentially drains the aquifers of the watershed, and a quick flow that is a direct result of the rainfall event. This conceptual approach involves the determination of reference points on an event hydrograph, i.e., the beginning and end of a rainfall event. The flow before and after these reference points is considered slow flow until the next hydrological event response. These assumptions are determined subjectively. Therefore, this approach essentially requires the user's experience and judgment. It is often less challenging to identify the beginning of an event than the end. Linsley et al. (1982) proposed the following empirical formulation to estimate the number of days (N) after the peak flow required for the direct runoff to cease:

$$N = A^{0.2} \tag{1}$$

where N is the time from the peak of the hydrograph to the point where direct runoff ceases (days), and A is the area of the watershed (mi^2).

Over the years, conceptual separation has been largely replaced by automated filtering approaches that were developed to standardize the conceptual methods for slow flow separation. They are simple methods that use only streamflow time series as input. The event hydrograph is the classic response to rainfall, and the previous low flow conditions in the stream are entirely related to slow flow until the end of the dry period. Low flow conditions have been widely studied, and instream minimum flows have been identified to be generally representative of slow flow. A well-known minimum smoothing method was developed by the Institute of Hydrology (1980). The method, originally called UKIH (for U.K. Institute for Hydrology) and later revised by Piggott et al. (2005), divides the time series into a sequence of five-day segments. The minimum flows are identified and selected by predetermined selection criteria. The slow flow hydrograph is then defined as the line connecting the minima. Some filters combine the quick runoff duration (eq. 1) with the local minimum approach (Sloto and Crouse, 1996) or with analysis of hydrograph recession curves (Rutledge, 1998). The HYSEP (Hydrograph Separation Program) by Sloto and Crouse (1996) uses the time window of quick runoff duration with three algorithms that include a fixed interval (FIXED), a sliding interval (SLIDE), and a local minimum (LOCMIN). The time window is calculated by doubling (or rounding) the empirically calculated runoff duration from equation 1 (Brodie and Hostetler, 2005). Within the predefined moving time window, successive minimum flows are identified on the streamflow hydrograph. The slow flow hydrograph is defined as the line connecting the minima.

Other filters are based on signal analysis techniques. Recursive analytical filters are used to remove the high-frequency signal of quick flow to obtain the lower-frequency signal of slow flow (Lyne and Hollick, 1979; Nathan and McMahon, 1990; Arnold and Allen, 1999). The degree of filtering is determined by the user by adjusting a coefficient and selecting the number of filter passes (Nathan and McMahon, 1990; Mau and Winter, 1997). It is difficult to objectively assess the accuracy of these filters, as the filtering process remains subjective. These methods are purely analytical in the sense that they are not based on physical processes. The major challenge for hydrologists is to develop algorithms that have a hydrological basis and can use physical parameters. Eckhardt (2005) introduced a general formulation, developed from several commonly used filters (Chapman, 1991; Chapman and Maxwell, 1996), based on the assumption of a linear aquifer reservoir. The recursive Eckhardt filter has two adjustable parameters related to the baseflow recession constant and the maximum baseflow index (BFI_{max}). The baseflow index is the long-term ratio of baseflow to total flow. The recession constant can be determined by analysis of hydrograph recession curves for segments of the hydrograph that are dominated by the release of water from natural storages, which are typically assumed to be groundwater discharge. Recession curves can be selected from the hydrograph and can be analyzed individually or collectively to better understand the flow processes that determine slow flow (Brodie and Hostetler, 2005). The partitioning method PART (Rutledge, 1998) finds the recording period for days that correspond to a requirement of antecedent recession, which indicates that the slow flow is equal to the streamflow on those days, and then linearly interpolates slow flow for the other days. The traditional approach to recession analysis has been graphical. It is often represented by a linear relationship between storage and outflow (Gonzales et al., 2009; Thomas et al., 2015). However, recession behavior can be complex, variable, and non-linear, and interpretation of the stream hydrograph requires a good hydrogeological understanding of the watershed.

Tracers and isotopes have been the most promising methods for obtaining the hydrogeological understanding required for the interpretation of stream hydrographs. They are based on an experimental approach that aims to understand the interaction between groundwater and surface water. Tracer-based hydrograph separation relies on the principle that the geochemical signature of water is determined by its hydrological pathway. The variation of streamflow electrical conductivity, which reflects the overall load of dissolved elements (soil mineral salts), has been mainly used (Pinder and Jones, 1969; Pilgrim et al., 1979; Matsubayashi et al., 1993; Stewart et al., 2007; Pellerin et al., 2008; Kronholm and Capel, 2015; Raffensperger et al., 2017). Surface runoff from a rain event has a direct and rapid pathway to the outlet and is therefore less exposed to salt dissolution. The slow flow pathway through the soil matrix facilitates the leaching of salts. Therefore, the level of electrical conductivity identifies the proportion of runoff from the ground (slow flow) and the surface (quick flow) at any time. Thus, variations in streamflow and conductivity represent a hydrogeochemical dynamic of a hydrological system in the watershed. Note that hydrograph separation with the geochemical method typically identifies two sources of streamflow: slow flow and quick flow. Streamflow and geochemical signature data must be measured simultaneously.

The use of multiple hydrograph separation methods is often recommended, as the accuracy of a single method is difficult to assess (Halford and Mayer, 2000). The methods give different separation results. Rutledge (2005) suggested that the traditional methods should be applied with care and appropriate consideration of the underlying assumptions of the method. Comparative studies to evaluate hydrograph separation methods (e.g., Nathan and McMahon, 1990; Arnold et al., 1995; Mau and Winter, 1997; Chapman, 1999; Halford and Mayer, 2000; Neff et al., 2005; Schwartz, 2007; Eckhardt, 2008) were often based on subjective measures, such as the plausibility of hydrological behavior, rather than a quantitative comparison to a known and well quantified baseflow hydrograph. Unfortunately, there are no clear indicators as to which separation methods are most or least appropriate for particular conditions, which is not surprising given the lack of a true physical basis for the methods (Partington et al., 2012). On the other hand, numerous studies (Stewart et al., 2007; Gonzales et al., 2009; Kronholm and Capel, 2015; Raffensperger et al., 2017) have shown how the application of different methods of hydrograph separation, combined with additional experimental investigations, can lead to better understanding of the processes involved in runoff generation. They have also shown how tracer separations could be used for validation.

In this respect, our study on hydrograph separation was undertaken with a focus on agricultural watersheds. There are many methods for separating hydrographs, but the complex behavior of agricultural drained watersheds is a topic that has not been widely investigated. To better understand the hydrological response of agricultural watersheds in Québec, the stream water electrical conductivity was used as a geochemical tracer. Because it is based on physical processes, hydrograph separation by the geochemical method was assumed to represent an accurate separation of the streamflow hydrograph into its two main components: quick flow and slow flow. The objective of this research was then to evaluate the performance of existing automated filtering methods for hydrograph separation (FIXED, SLIDE, LOCMIN, PART, UKIH, BFLOW, and Eckhardt). The geochemical method was used as a reference for comparison with the filtering methods.

Methods and Materials

Watershed Descriptions

Hydrometric time series data from 14 small watersheds monitored by the Institut de Recherche et de Développement en Agroenvironnement (IRDA) were used for this study. Figure 1 locates the experimental sites in the province of Québec, Canada. They were organized into twin experimental subwatersheds (fig. 2), identified as upstream and downstream, to study diffuse phosphorus exports from agricultural areas (Beaudin et al., 2006; Michaud et al., 2009a, 2009b). Upstream refers to a subwatershed in which specific agricultural management practices were applied, while management practices were limited in downstream subwatersheds. Agricultural management practices in the upstream subwatersheds were implemented to limit erosion and sediment transport. The erosion was the result of poor surface drainage, where excessive runoff water was discharged without proper protection of streambanks. The rounded and narrow trenches, combined with shallow ditches, increased the problem of runoff concentration. To ensure efficient drainage of surface runoff to the stream, grassed waterways and openings were created at the outlets of ditches or depressions. A few collection ponds equipped with gutters were created at the outlets of ditches with a high potential for sediment transport to reduce export to the stream. Specific streambank protection measures also included reducing the slope of some unstable embankments, planting vegetation on the banks, stabilizing degraded embankment sections using

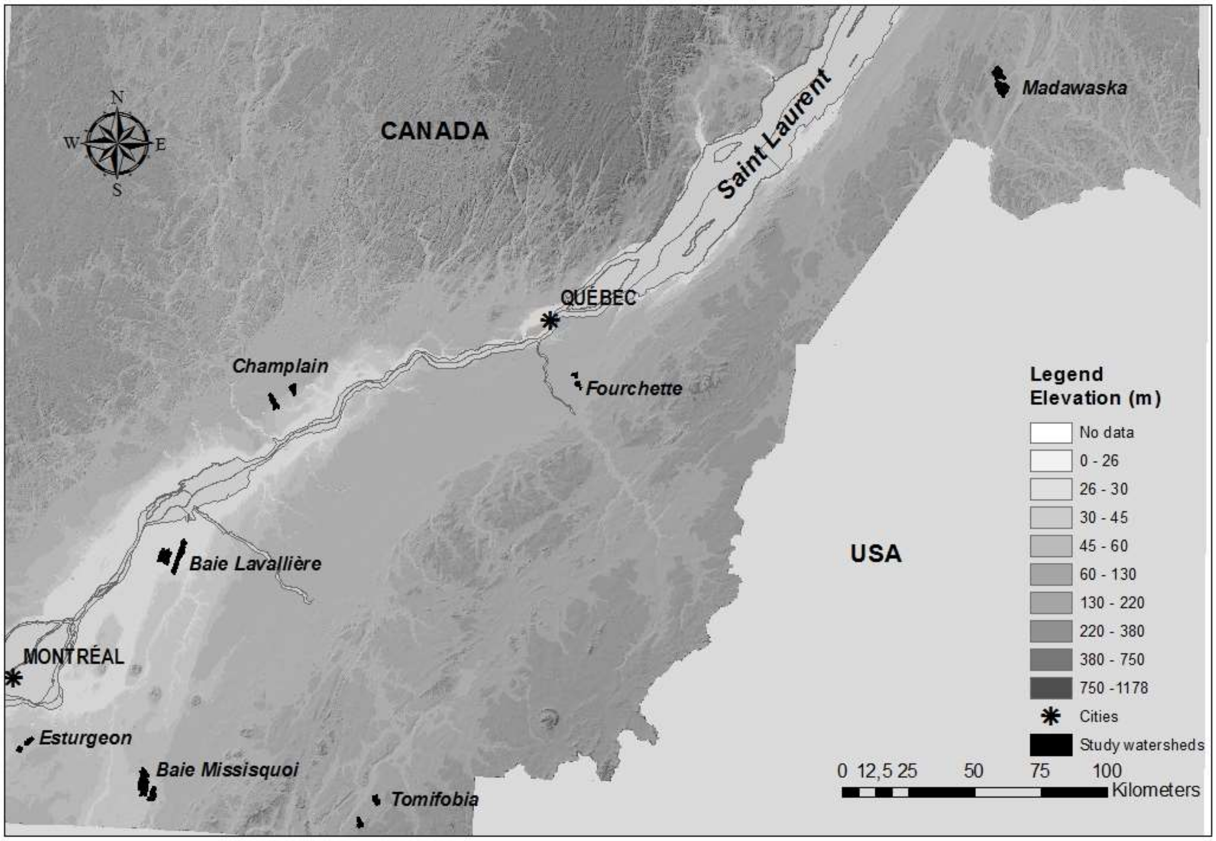

Figure 1. Location of experimental sites in the province of Québec.

plant-based erosion techniques, and establishing riparian strips on all streambanks. Tree species have been preferred to establish shelterbelts.

In addition, these subwatersheds have undergone substantial changes related to surface and subsurface (tile) drainage practices (table 1). The role of tile drainage is to drain soils that are seasonally wet and to lower groundwater tables that are effectively of shallow depth. Surface drainage, particularly in flat areas, is designed to ensure uniform distribution of water, improve infiltration, and discharge surface runoff into the drainage network. Surface drainage is

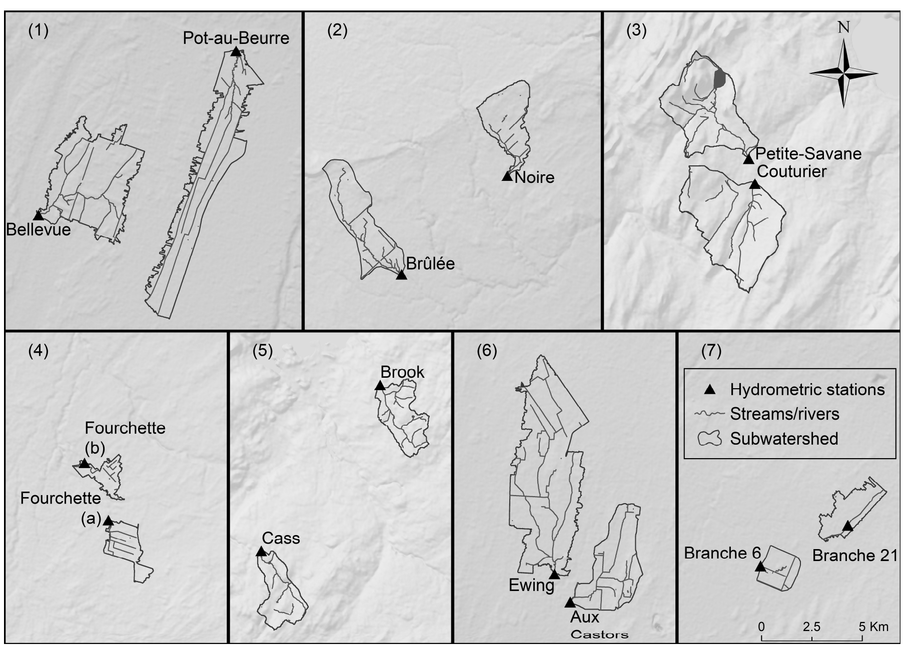

Figure 2. Experimental setup of twin subwatersheds at each site: (1) Baie Lavallière, (2) Champlain, (3) Madawaska, (4) Fourchette, (5) Tomifobia, (6) Baie Missisquoi, and (7) Esturgeon.

Table 1. Summary description of watersheds and subwatersheds.

Regions	Watersheds	Subwatersheds	Area (km^2)	Rainfall (mm $year^{-1}$)	Relief	Soil Drainage Class[a] (% poor)	Subsurface Drainage[b] (% tile-drained)
Bas-Saint-Laurent	Madawaska	Couturier[c]	18.8	856	Steep	10	<40
		Petite Savane[d]	15.2			0	<40
Beauce	Fourchette	Fourchette[c]	2.5	1025	Hilly	10	40 to 80
		Fourchette[d]	1.9			25	40 to 80
Mauricie	Champlain	Brûlée[c]	9.6	983	Hilly	78	40 to 80
		Noire[d]	8.2			40	40 to 80
Montérégie - Est	Baie Lavallière	Pot-au-Beurre[c]	20.1	1040	Flat	93	>80
		Bellevue[d]	16.1			56	>80
Montérégie - Est	Baie Missisquoi	Ewing	33.2	970	Lowlands	36	>80
		Aux Castors	11.2			29	>80
Montérégie - Ouest	Esturgeon	Branche 6[c]	3.2	1159	Very flat	96	>80
		Branche 21[d]	2.3			98	>80
Estrie	Tomifobia	Cass[c]	6.2	1269	Steep	9	<40
		Brook[d]	7.2			35	<40

[a] Ratio of area of poorly drained soils to the total area of the subwatershed.
[b] Ratio of area of tile-drained soils to the total area of the subwatershed.
[c] Upstream subwatershed.
[d] Downstream subwatershed.

more important than subsurface drainage to effectively remove water from post-winter snowmelt. Snowmelt occurs in the spring, which corresponds to the thawing period of the soil. At the end of the thawing period, water accumulated in depressions infiltrates and reaches the groundwater table, bringing it closer to the soil surface. The groundwater table is generally near the surface in early spring, drops significantly during the summer, and then rises again in the fall. Subsurface drainage fulfills its role when the groundwater table is so high (Muma et al., 2016). The agricultural drainage system safely discharges excess surface and subsurface water from fields through appropriate structures (canals, ditches, etc.) while preventing erosion. A detailed description of the watersheds is provided in the Appendix.

Data Availability

Year-round hydrometric monitoring protocols were identical for all 14 subwatersheds. These protocols are described more fully by Michaud et al. (2009b, 2009c, 2012). The hydrometric stations were equipped with barometric, acoustic, and multi-parameter probes continuously recording the water stage, velocity, conductivity, turbidity, and temperature. Discharge calibration curves were derived from monthly streamflow monitoring using Doppler or propeller current meters with a minimum of 15 velocity measurements in the stream cross-section. Hydrograph separation was conducted on the data sets of different periods (table 2), excluding winter (January and February) when the multi-parameter probes were removed to prevent breakdown due to cold temperature. Streamflow and electrical conductivity data were available at 15 min intervals. Hydrograph separation methods were applied on a daily basis. Data were aggregated accordingly.

Geochemical Method

The geochemical hydrograph separation method applied on streamflow and electrical conductivity time series is based on the principle of dilution where the equations of continuity and mass balance lead to contribution ratios (Matsubayashi et al. 1993). The mass balance equations are as follows:

$$Q_t = Q_q + Q_s \quad (2)$$

$$C_t Q_t = C_q Q_q + C_s Q_s \quad (3)$$

$$Q_s / Q_t = \left(C_t - C_q\right) / \left(C_s - C_q\right) \quad (4)$$

where
Q_t = total streamflow (mm d^{-1})
C_t = total streamflow electrical conductivity (μS cm^{-1})
Q_q = quick flow (mm d^{-1})
C_q = quick flow electrical conductivity (μS cm^{-1})
Q_s = slow flow (mm d^{-1})
C_s = slow flow electrical conductivity (μS cm^{-1}).

Equation 4 calculates the contribution of slow flow, combining the contributions of tile drainage and shallow aquifer discharge. Tile flow includes a volume of water drained from the soil in which the mineralization is close to that of groundwater. To perform geochemical hydrograph separation, the

Table 2. Recording periods (day/month) of streamflow and electrical conductivity data on each site (ND = no data).[a]

Year	Madawaska CO, PS	Fourchette FU, FD	Champlain BU, NO	Baie Lavallière PB, BE	Baie Missisquoi EW	Baie Missisquoi CA	Esturgeon BR6, BR21	Tomifobia CS, BO
2005	ND	ND	ND	ND	ND	15/4 to 5/11	ND	ND
2006	ND	ND	ND	ND	ND	2/4 to 16/10	ND	ND
2007	ND	27/3 to 19/11	ND	ND	28/6 to 21/11	9/7 to 12/11	ND	ND
2008	ND	8/4 to 19/11	ND	ND	1/4 to 10/12	13/5 to 24/11	ND	ND
2009	3/11 to 7/12	31/3 to 8/12	15/10 to 10/12	1/6 to 10/12	25/3 to 10/12	29/4 to 26/11	25/9 to 11/12	23/9 to 10/12
2010	18/3 to 30/11	17/3 to 25/11	19/3 to 24/11	10/3 to 24/11	31/3 to 23/11	15/4 to 3/11	17/3 to 23/11	18/3 to 22/11
2011	29/4 to 28/9	07/4 to 23/11	22/3 to 22/11	17/3 to 13/11	30/3 to 09/11	29/3 to 8/11	21/4 to 24/11	15/3 to 3/10

[a] Sites are Couturier (CO), Petite Savane (PS), Fourchette upstream (FU), Fourchette downstream (FD), Brûlée (BU), Noire (NO), Pot-au-Beurre (PB), Bellevue (BE), Ewing (EW), Aux Castors (CA), Branche 6 (BR6), Branche 21 (BR21), Cass (CS), and Brook (BO).

quick flow conductivity (C_q) and slow flow conductivity (C_s) must be determined. The hydrograph separation relied on three assumptions: (1) C_q was equal to the lowest observed conductivity value, (2) C_s was equal to pre-event conductivity, considering the absence of quick flow preceding the hydrological response to precipitation, and (3) C_s and C_q remained constant over the entire recording period.

In this study, events occurring after at least one week (seven consecutive days) without precipitation were identified, and their initial conductivity values were recorded to determine C_s. An average value was then calculated for each subwatershed, referred to as C_s. Thus, as soon as the streamflow conductivity was equal to or greater than C_s, the streamflow was treated as slow flow. This value was therefore assumed to be representative of 100% slow flow conditions in the stream. To estimate C_q, a selection of the lowest observed conductivity values was performed; these values occurred during peak flows, i.e., when the contribution of quick flow was at its maximum. Conductivity decreased as the streamflow increased due to dilution of stream water with low mineralized rainwater. It was assumed that the low conductivity represented 100% quick flow conditions in the total flow. For each subwatershed, the lowest conductivity value was used for C_q. Note that the C_q values obtained were limited to the databases used for this study.

Filtering Methods

FIXED, SLIDE, and LOCMIN are techniques developed by Pettyjohn and Henning (1979), as implemented by Sloto and Crouse (1996). These techniques apply a predefined moving time window to find successive minimum streamflow values during an interval $2N^*$ days (N from eq. 1). The width of the interval $2N^*$ used for hydrograph separation is the nearest odd integer (between 3 and 11) to twice the value of N (Pettyjohn and Henning, 1979). The asterisk (*) signifies that the interval is not exactly equal to twice the value of N. FIXED assigns the lowest streamflow in the interval $2N^*$ to all days, starting with the first day of the streamflow record. The analysis is then moved forward $2N^*$ days, and the process is repeated. SLIDE centers the interval $2N^*$ on the day of interest. Slow flow for that day is assigned the minimum streamflow within the interval. The interval is then moved forward one day, and the process is repeated. LOCMIN centers the interval $2N^*$ on the day of interest. If it is the minimum streamflow within the interval, it is assigned as a local minimum. Slow flow for days between local minima is estimated by linear interpolation.

UKIH (Piggott et al. 2005) is based on the identification and interpolation of turning points within streamflow time series. The turning points indicate the days and corresponding streamflow values when the observed flow is assumed to be entirely slow flow. To calculate the turning points, the streamflow data are partitioned into a sequence of five-day segments, and the minimum values of streamflow within each segment (an x and y pair where xi is the day on which the minimum flow occurred, and yi is the minimum flow value) are selected and defined as candidate turning points. Each candidate is then compared to the minima for the previous and subsequent segments. Turning points are defined when the condition $0.9yi < \min(yi\text{-}1,\ yi\text{+}1)$ is satisfied. The temporal variation of slow flow is estimated by piecewise linear interpolation bracketed by successive pairs of turning points.

PART (Rutledge, 1998) finds days of slow flow in the days following an event that meet a requirement for antecedent recession. For a given day, the antecedent recession requirement is met if recession has been continuous for N (eq. 1) days or more preceding the day and the rate of recession is less than 0.1 log cycle per day. PART uses linear interpolation to connect across periods that do not meet the fixed conditions.

The Arnold and Allen (1999) recursive filter (BFLOW) is a variant of the algorithm of Lyne and Hollick (1979) commonly used in signal analysis and processing. The separation technique consists of filtering out high-frequency signals of quick flow from low-frequency baseflow (slow flow). The filter is of the following simple form:

$$Qf_i = \beta Qf_{i-1} + \frac{1+\beta}{2}\left(Q_i - Q_{i-1}\right) \tag{5}$$

$$Qb_i = Q_i - Qf_i \tag{6}$$

where
Q_i = total streamflow on day i (mm d^{-1})
Q_{i-1} = total streamflow on previous day (mm d^{-1})
Qf_i = filtered quick flow on day i (mm d^{-1})
Qf_{i-1} = filtered quick flow on previous day (mm d^{-1})
Qb_i = slow flow on day i (mm d^{-1})
β = filter parameter (β = 0.925).

Nathan and McMahon (1990) determined 0.925 as the optimum value for β. They indicated that the value of the filter parameter that provided the most acceptable baseflow separation was in the range of 0.9 to 0.95.

The filter of Eckhardt (2005) is used to perform low-pass filtering on the hydrograph to separate slow flow. The filter equation is:

$$Qb_i = \frac{\left[\left(1-\mathrm{BFI}_{max}\right)aQb_{i-1} + \left(1-a\right)\mathrm{BFI}_{max}Q_i\right]}{\left(1-a\mathrm{BFI}_{max}\right)} \tag{7}$$

where
Q_i = total streamflow on day i (mm d^{-1})
Qb_i = slow flow on day i (mm d^{-1})
Qb_{i-1} = slow flow on previous day (mm d^{-1})
BFI_{max} = long-term ratio of slow flow
a = recession constant.

This recursive filter requires the determination of two parameters: (1) the recession constant a, and (2) the long-term ratio of slow flow BFI_{max} (maximum value of the baseflow index). The BFI_{max} parameter cannot be measured but can be obtained from predefined values based on different types of aquifers. Eckhardt (2005) suggested setting BFI_{max} to 0.80 for perennial streams with porous aquifers, 0.50 for ephemeral streams with porous aquifers, and 0.25 for perennial streams with hard rock aquifers. Eckhardt (2005) also recommended using tracer data to calibrate the BFI_{max} parameter. In this study, BFI_{max} was calibrated using the geochemical method. The recession constant (a) was obtained by selecting several recession segments to find an average recession value for each subwatershed.

The application of FIXED, SLIDE, LOCMIN, UKIH, PART, and BFLOW did not require any special procedure for calibration. Hence, they are categorized as non-calibrated filters in this article.

Calibration of Eckhardt Filter

To identify optimum values of BFI_{max}, an automatic calibration was performed between geochemical and Eckhardt slow flow components. The shuffle complex evolution (SCE) optimization tool (Duan et al., 1993) was used to minimize the following objective function (Coron et al., 2012):

$$\varepsilon = \text{RMSE}\left(\sqrt{Q}\right)\left(1+\left|\text{BIAS}\right|\right) \quad (8)$$

$$\text{RMSE} = \sqrt{\frac{1}{n}\sum_{i=1}^{n}\left(Q_i^{sim} - Q_i^{obs}\right)} \quad (9)$$

$$\text{BIAS} = \frac{\sum_{i=1}^{n}\left(Q_i^{sim} - Q_i^{obs}\right)}{\sum_{i=1}^{n}\left(Q_i^{obs}\right)} \quad (10)$$

where

Q_i^{obs} = geochemical observed slow flow on day i (mm d^{-1})

Q_i^{sim} = Eckhardt simulated slow flow on day i (mm d^{-1})

n = number of observations.

The combination of RMSE and BIAS, as proposed by Coron et al. (2012), gives weight to dynamic representation as well as water balance. Using square root transformed flows to compute the RMSE reduces the influence of high flows during calibration and was found to give a better compromise between the different criteria (Coron et al., 2012).

The Nash-Sutcliffe efficiency coefficient (NSE), Pearson correlation coefficient (R), percentage bias (PBIAS) difference, and RMSE (Moriasi et al., 2007) were used as statistical measures of model performance. They assessed the relative difference between the observed geochemical slow flow and simulated Eckhardt slow flow estimates:

$$\text{R} = \frac{\sum_{i=1}^{n}\left(Q_i^{obs} - Q_{mean}^{obs}\right)\left(Q_i^{sim} - Q_{mean}^{sim}\right)}{\sqrt{\sum_{i=1}^{n}\left(Q_i^{obs} - Q_{mean}^{obs}\right)^2}\sqrt{\sum_{i=1}^{n}\left(Q_i^{sim} - Q_{mean}^{sim}\right)^2}} \quad (11)$$

$$\text{NSE} = 1 - \left[\frac{\sum_{i=1}^{n}\left(Q_i^{obs} - Q_i^{sim}\right)^2}{\sum_{i=1}^{n}\left(Q_i^{obs} - Q_{mean}^{obs}\right)^2}\right] \quad (12)$$

$$\text{PBIAS} = \left[\frac{\sum_{i=1}^{n}\left(Q_i^{obs} - Q_i^{sim}\right)\times 100}{\sum_{i=1}^{n}\left(Q_i^{obs}\right)}\right] \quad (13)$$

where

Q_i^{obs} = geochemical observed slow flow on day i (mm d^{-1})

Q_i^{sim} = Eckhardt simulated slow flow on day i (mm d^{-1})

Q_{mean}^{obs} = geochemical observed mean slow flow (mm d^{-1})

Q_{mean}^{sim} = Eckhardt simulated mean slow flow (mm d^{-1})

n = number of observations.

Two options were considered for calibrating BFI_{max}, and their applications were used to determine the appropriate option for the study sites. The first option aimed to use a single BFI_{max} value for each watershed's upstream and downstream sites, given that the upstream and downstream subwatersheds are close to each other and assuming that they have identical aquifer characteristics. The upstream subwatersheds were then selected for calibration, while the downstream subwatersheds were used for validation. The calibration period was the year 2010, and the validation period was 2011, both common to all paired experimental sites. For the second option, BFI_{max} values were identified for each subwatershed, and the calibration and validation periods varied according to the data available (table 2) for each site. Thus, for Fourchette (upstream and downstream) and Ewing, the calibration periods were from 2007 to 2009. While for Aux Castors, the calibration periods were from 2005 to 2009. The validation periods for these four sites included 2010 and 2011. For the ten remaining sites, the calibration period was 2009 and 2010, with only one period (2011) available for validation.

Filter Evaluation

Evaluation of each of the seven methods was based on each site's geochemical hydrograph separation results. In addition to visual analysis of the slow flow hydrographs, the calculated slow flow fractions were used to examine the performance of each filter hydrograph separation in a given period. The slow flow fraction for any given length of time was calculated as:

$$\text{slow flow fraction} = \sum_{i=1}^{n}Q_i^{s} \Big/ \sum_{i=1}^{n}Q_i^{t} \quad (14)$$

where

Q_i^{s} = slow flow on day i (mm d^{-1})

Q_i^{t} = total streamflow on day i (mm d^{-1})

n = number of observations.

Quick flow was calculated as the difference between total flow and slow flow. Analysis of the hydrograph separation for each site was supported by daily precipitation data. These data were simply visualized to interpret daily, seasonal, and inter-annual variations of the observed water balances.

Evaluation of the non-calibrated filters using the geochemical method was completed by statistical analysis. Evaluation of the calibrated Eckhardt filter results was limited to the statistical measures of model performance listed in the previous section on calibration. It was assumed that the slow flow separation of the Eckhardt filter after calibration was in agreement with that of the geochemical method.

STATISTICAL ANALYSIS

Data were modeled using a multivariate analysis of variance (MANOVA) model with repeated measurements. The fixed effects included the following factors: watershed relief, subwatershed status, year, season, method, and all second-order interaction terms. Watershed relief was classified as hilly or flat, representing the main landscapes of the study watersheds. The description “hilly” referred to both hilly and steep landscapes, while “flat” included lowlands and flat landscapes. The subwatershed status factor represented the twin subwatersheds (upstream and downstream). The year factor included 2010 and 2011, which were common to all watersheds. The season factor was based on three seasons (spring, summer, and fall) that covered the geochemical data monitoring period. Spring was April and May, summer was June to August, and fall was September to November. A monthly time step was applied for the slow flow variable; the months included the geochemical data monitoring period from April to November for each year.

The dependency between observations taken on the same subwatershed was considered in the MANOVA model. In fact, an unstructured correlation was fitted to observations from different methods, while a first-order autoregressive structure of correlation was fitted to observations from different months. Following any significant effect in the model, the post-hoc Tukey-Kramer comparison method was used to see where the differences occurred. All data met assumptions of normality and homogeneity of variances, but sometimes a transformation of the response variable was required. All analyses were performed using SAS (ver. 9.4, SAS Institute, Cary, N.C.) at the 0.05 level of significance.

RESULTS

GEOCHEMICAL HYDROGRAPH SEPARATION

Geochemical hydrograph separation was performed at all sites based on equation 4, applying the electrical conductivity values from table 3. Quick flow conductivities (C_q) and slow flow conductivities (C_s) for the 14 sites averaged to 0.046 and 0.668 μS cm^{-1}, respectively. The highest average values of slow flow conductivity were observed in the Esturgeon subwatersheds: Branche 6 (0.919 μS cm^{-1}) and Branche 21 (1.169 μS cm^{-1}). The high concentration of soluble salts in organic soils distinguishes them from the other experimental watersheds, mainly agricultural mineral soils. Figure 3 illustrates the streamflow and its slow flow component derived from the electrical conductivity for 25 March to 10 December 2009 at Ewing outlet. The minimum electrical conductivity (C_q) values in table 3 often occurred during periods of high flows generated by snowmelt, when the largest fraction was from quick flow.

Table 3. Parameter values of electrical conductivity of quick flow (C_q) and slow flow (C_s) at each site.[a]

	Madawaska		Fourchette		Champlain		Baie Lavallière		Baie Missisquoi		Esturgeon		Tomifobia	
Parameter	CO	PS	FU	FD	BU	NO	PB	BE	EW	CA	BR6	BR21	CS	BO
C_q	0.031	0.021	0.041	0.005	0.031	0.027	0.065	0.025	0.037	0.045	0.087	0.070	0.037	0.051
C_s	0.167	0.604	0.632	0.242	0.197	0.483	0.823	0.522	0.722	0.810	0.919	1.169	0.352	0.409

[a] Sites are Couturier (CO), Petite Savane (PS), Fourchette upstream (FU), Fourchette downstream (FD), Brûlée (BU), Noire (NO), Pot-au-Beurre (PB), Bellevue (BE), Ewing (EW), Aux Castors (CA), Branche 6 (BR6), Branche 21 (BR21), Cass (CS), and Brook (BO).

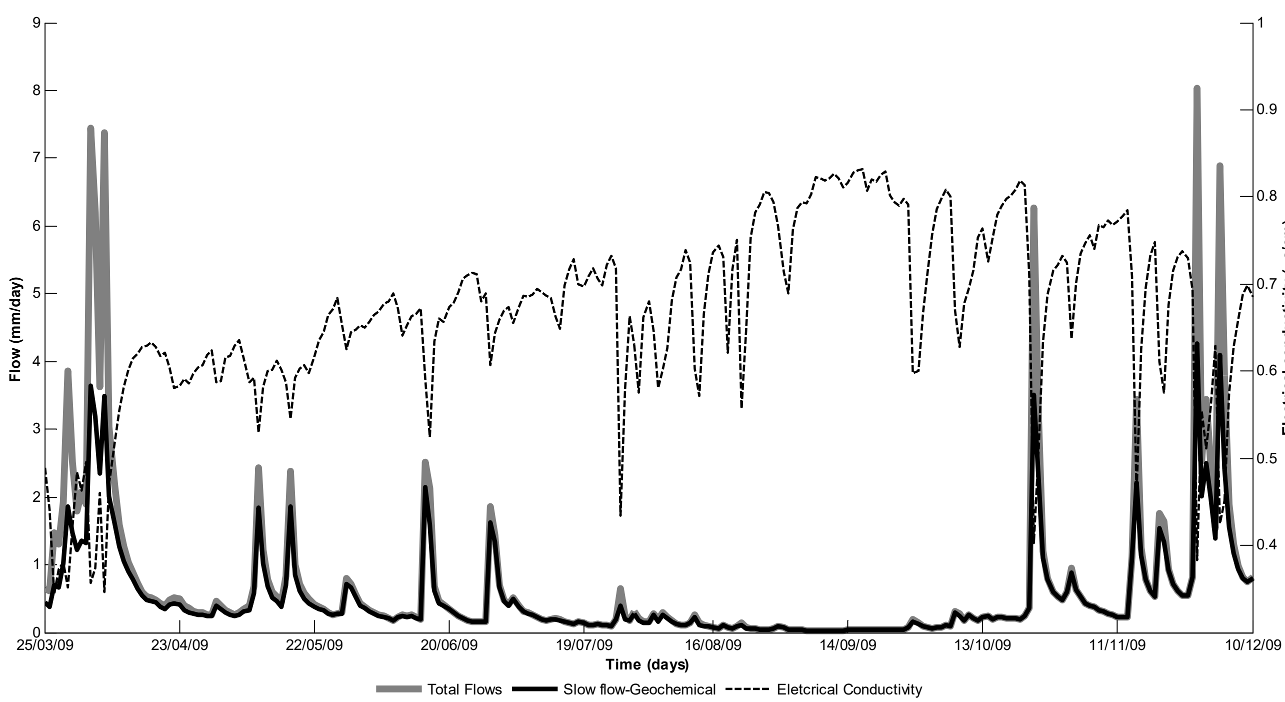

Figure 3. Daily slow flow hydrograph separation based on conductivity and total streamflow from 25 March to 10 December 2009 on Ewing.

Runoff events associated with snowmelt in April and higher precipitation in late fall showed an increase in the total water discharged at the subwatershed outlet (fig. 3). In particular, this resulted in a high contribution of quick runoff. Otherwise, implementation of a subsurface drainage system generally leads to a reduction in quick runoff by increasing the infiltration of precipitation. The tiles route a portion of the slow runoff (flowing from the soil) toward the stream, resulting in a decrease in the water stored in the soil profile and an increase in slow runoff. A subsurface drainage network generally reduces the response time of agricultural plots. This leads to hydrographs of hydrological events with a sharp rise and a steep slope of recession, known as flashy hydrographs. The results of the geochemical method during the hydrological events indicated that the slow flow increased and decreased in a manner that roughly matched the peaks of the streamflow (fig. 3). Typically, the recession segments started with a steep curve that represented flashier drainage of the subsurface tiles, ending with a gradually decreasing curve that reflected the contribution of delayed slow flows, mainly from the shallow aquifer. Tile flows contribute to the streamflow in the form of soil water and/or release from the shallow aquifer. Between runoff events, streamflow is mainly slow flow from the tiles and shallow aquifer connected to the stream.

Table 4 presents the water depths exported to the outlets, quick runoff, and slow flow for the twelve experimental subwatersheds for the common period of 2010 and 2011. The results from Baie Missisquoi watershed are not included because they are presented later using several years of observations. Overall, the exported water depths were highly variable across the study areas, ranging from a minimum of 133 mm at Branch 6 (Esturgeon) to 546 mm at Brook (Tomifobia) over the period of April to November. These variations reflect the interaction of several factors, including the spatial distribution of precipitation, the amount of snow cover, soil and landscape properties, as well as land use and land management.

The quick and slow responses from the 12 subwatersheds were significantly different from 2010 to 2011, and the slow flow fractions were systematically lower in 2011. Due to wetter and more frequent events, the quick flow contributions were substantially higher in 2011, in addition to a spring characterized by strong snowmelt. Analysis of table 4 also indicates that quick flow processes were more intense in the downstream subwatersheds than in the upstream subwatersheds. In the Champlain subwatersheds, for example, the contribution of quick runoff to total flow was 42% (Noire) and 18% (Brûlée) in 2010 and 59% and 33%, respectively, in 2011. Hydropedological factors would explain the gradient observed in the proportions of quick flow; 20% of downstream (Noire) soils have a clayey or clay loam texture related to slow permeability, and this proportion is only 12% upstream (Brûlée). Note that more significant quick runoff occurred in Noire despite the larger pasture area (63% of the cultivated area) than in Brûlée (40%). These observations indicate a stronger influence of soil properties than crop rotations on the water balance in this area. Similarly, the influence of soil properties on the water balance was even more pronounced in the Tomifobia subwatersheds. On Cass (upstream), the good quality of the natural drainage contributed to the limited intensity of quick flow (20% to 35%) despite the steep landscape with an average slope of 6.7%. In the adjacent twin subwatershed of Brook (downstream), due to the low natural permeability of the soils, quick flow varied by 32% and 47% of total water yield for 2010 and 2011, respectively.

In the Esturgeon subwatersheds, hydrometric monitoring of Branche 6 showed a particular hydrological regime for the black soil. While the total stream water depth was only 133 mm, only 29 mm of this depth was quick flow in 2010. The physical properties of the organic soil, including its high water retention and irrigation-based water management, contributed to this low ratio of quick runoff (22% of total flow). The downstream subwatershed (Branche 21) was more subjected to quick flow than the upstream subwatershed, with 35% in 2010 and 50% in 2011.

The exported water depths and relative proportions of quick runoff were significantly reduced in the Baie Lavallière watersheds. On the flat landscape of Pot-au-Beurre (upstream) with intensive cropping systems, the contribution of slow flow was an average of 75% of the total flow (table 4). In the Bellevue subwatershed (downstream), the contribution of slow flow averaged 56%. More permeable topsoils in Pot-au-Beurre and efficient subsurface drainage systems over a larger cultivated area than in Bellevue presumably explain the difference in flow partitioning between these subwatersheds.

In the Madawaska subwatersheds, quick runoff represented 42% (2010) and 58% (2011) of the total stream water

Table 4. Streamflow partitioning in the 12 subwatersheds into quick and slow flow in 2010 and 2011.[a]

		Madawaska		Fourchette		Champlain		Baie Lavallière		Esturgeon		Tomifobia	
Year	Flow	CO	PS	FU	FD	BU	NO	PB	BE	BR6	BR21	CS	BO
2010	Data length (days)	257	257	253	253	238	250	244	221	251	251	249	249
	Streamflow (mm)	467	422	423	446	365	295	298	244	133	412	491	546
	Quick flow (mm)	167	176	143	157	58	149	58	104	29	143	99	175
	Slow flow (mm)	299	245	280	289	307	146	240	141	104	270	392	372
	Slow flow fraction[b]	0.64	0.58	0.66	0.65	0.84	0.49	0.81	0.58	0.78	0.65	0.80	0.68
2011	Data length (days)	168	180	230	230	231	207	186	199	160	197	193	198
	Streamflow (mm)	428	451	611	639	726	506	377	423	97	388	592	628
	Quick flow (mm)	177	262	300	305	243	298	115	196	33	196	206	294
	Slow flow (mm)	251	189	311	334	483	209	262	227	64	192	386	334
	Slow flow fraction[b]	0.59	0.42	0.51	0.52	0.67	0.41	0.69	0.54	0.66	0.50	0.65	0.53

[a] Sites are Couturier (CO), Petite Savane (PS), Fourchette upstream (FU), Fourchette downstream (FD), Brûlée (BU), Noire (NO), Pot-au-Beurre (PB), Bellevue (BE), Ewing (EW), Aux Castors (CA), Branche 6 (BR6), Branche 21 (BR21), Cass (CS), and Brook (BO).

[b] Fraction of total streamflow.

depths exported from Petite Savane, compared to 37% (2010) and 41% (2011) in Couturier. This was strongly related to the significantly steeper terrain in Petite Savane than in Couturier. There was also much less agricultural activity in Petite Savane (20%) than in Couturier (41%).

The streamflow separation in Fourchette showed similar slow flow partitions in both the upstream (66% in 2010, 51% in 2011) and downstream (65% in 2010, 52% in 2011) subwatersheds, despite less intensive land use downstream, with more forest cover (38%) than upstream (8%). The downstream subwatershed occupies a lower position in the watershed landscape, and its outlet is 15 m lower than the upstream subwatershed.

Table 5 presents the total, slow, and quick water depths in the Baie Missisquoi subwatersheds (Ewing and Aux Castors), both sites having longer periods of record (5 and 7 years, respectively). More surface runoff has been observed on Ewing despite the high water depth exported over Aux Castors, although the two sites have similar landscapes and land use. Table 5 shows significant inter-annual variability in water yields and streamflow partitioning. For example, at Ewing, the lowest slow flow fraction of 52% was observed in 2011 and the highest value was 75% in 2009. The unusually heavy rainfall in fall 2011 provided significant contributions of quick flow, compared to moderate rainfalls in 2009. Quick flow was particularly dominant in fall 2007, spring 2008, as well as in response to the exceptionally heavy rainfall in summer 2008. In addition, the abundant precipitation in fall 2005 (Hurricane Katrina) as well as in the spring and fall of 2006 explain the hydrological responses on Aux Castors (Michaud et al., 2009c). Averaged over the years, slow flow contributions were lower during the spring snowmelt period in April and May and higher during the summer from June to September (table 6).

Snowmelt-driven runoff events and late fall precipitation largely contributed to the increase of quick flows during the spring and fall, respectively. This highlights the influence of wetness conditions (antecedent soil moisture) and high-intensity rainfall that increase the generation of quick runoff.

The interactions between quick flow and slow flow varied significantly based on the local hydropedological interpretation of soils. Where the soil was more conductive, slow flow was significantly larger than quick flow. In less conductive soils, quick flow was larger than slow flow. A practical implication of the overall observations is that the local variability in flow partitioning, due to physiographic attributes, soil drainage capacity, and agricultural management practices, is relatively important and must be considered together with the largest-scale agro-climatic gradient when assessing the hydrological components of a given area.

Table 6. Seasonal streamflow partitioning for Ewing (EW) and Aux Castors (CA) over the April to November period.

	Streamflow (mm)		Quick Flow (mm)		Slow Flow (mm)		Slow Flow Fraction[a]	
Season	EW	CA	EW	CA	EW	CA	EW	CA
Spring	117	120	56	54	61	66	0.52	0.55
Summer	54	66	11	14	43	52	0.80	0.79
Fall	73	85	26	35	47	50	0.64	0.59

[a] Fraction of total streamflow.

FILTER HYDROGRAPH SEPARATION

Comparison of Non-Calibrated Filters to Geochemical Method

Table 7 compares the slow flow fractions estimated by the non-calibrated filters and geochemical method for 2010 and 2011. For individual sites, the slow flow fraction ranged from a low of 0.17 (BFLOW in 2010 at Branche 6 and UKIH in 2011 at Branche 21) to a high of 0.75 (SLIDE in 2010 at Fourchette downstream and FIXED in 2011 at Petite Savane). There was a large variation in the slow flow fractions between methods and over the years presented. The differences between the slow flow hydrographs from the non-calibrated filters and geochemical method are further detailed for the Ewing subwatershed for the 2007 and 2008 periods in figure A1 in the Appendix. Visual analysis of the hydrographs showed attenuated and relatively flat slow flow responses from the BFLOW and UKIH methods.

One cause of the differences between the hydrographs and slow flow fractions for the filtering methods was related to how each method quantified slow flow. The quick flow duration calculated from equation 1 for FIXED, SLIDE, and LOCMIN identified a quick flow that generally ceased between one to three days following an event. The daily slow flow separation of FIXED and SLIDE was based on a series of straight lines and steps. A single value was assigned to the entire interval that was physically unrealistic and sometimes overestimated the slow flow values compared to the geochemical values. On the other hand, the daily slow hydrographs of LOCMIN were characterized by interconnected straight lines, and the interpolation between local minima considerably reduced the contribution of slow flow. The UKIH method was similar to the LOCMIN method; linear interpolation between each turning point estimated the daily values of slow flow. Indeed, UKIH's five-day interval significantly underestimated the contribution of slow flow. The quick flow duration from these methods was much higher

Table 5. Streamflow partitioning for Ewing (EW) and Aux Castors (CA) into quick and slow flows for 2005 to 2011 (ND = no data).

Period	Year	Precipitation (mm)[a]	Streamflow (mm) EW	Streamflow (mm) CA	Quick Flow (mm) EW	Quick Flow (mm) CA	Slow Flow (mm) EW	Slow Flow (mm) CA	Slow Flow Fraction[b] EW	Slow Flow Fraction[b] CA
April to November	2005	986	ND	353	ND	111	ND	243	ND	0.69
April to October	2006	1109	ND	328	ND	132	ND	196	ND	0.60
July to November	2007	851	134	152	34	48	100	104	0.74	0.69
April to November	2008	816	308	321	128	107	180	214	0.59	0.67
April to November	2009	768	148	182	33	49	115	133	0.78	0.73
April to November	2010	890	256	270	82	97	174	173	0.68	0.64
April to November	2011	942	387	484	172	229	215	255	0.56	0.53

[a] Precipitation for each year is for April to November.
[b] Fraction of total streamflow.

Table 7. Slow flow fractions from non-calibrated filters and geochemical method in the 14 subwatersheds for 2010 and 2011.[a]

		Madawaska		Fourchette		Champlain		Baie Lavallière		Baie Missisquoi		Esturgeon		Tomifobia	
Year	Method	CO	PS	FU	FD	BU	NO	PB	BE	EW	CA	BR6	BR21	CS	BO
2010	BFLOW	0.27	0.33	0.30	0.36	0.29	0.26	0.28	0.26	0.23	0.21	0.17	0.22	0.39	0.33
	PART	0.55	0.63	0.65	0.75	0.57	0.52	0.61	0.44	0.48	0.49	0.27	0.37	0.66	0.53
	UKIH	0.28	0.45	0.31	0.38	0.35	0.31	0.30	0.27	0.32	0.32	0.20	0.22	0.44	0.36
	FIXED	0.67	0.61	0.66	0.76	0.61	0.60	0.68	0.54	0.47	0.46	0.39	0.43	0.65	0.52
	LOCMIN	0.52	0.57	0.56	0.68	0.43	0.39	0.48	0.38	0.37	0.35	0.23	0.32	0.58	0.49
	SLIDE	0.70	0.62	0.65	0.75	0.62	0.60	0.67	0.54	0.25	0.22	0.38	0.43	0.65	0.53
	Geochemical	0.63	0.66	0.67	0.65	0.81	0.51	0.80	0.63	0.67	0.62	0.74	0.62	0.80	0.68
2011	BFLOW	0.33	0.27	0.29	0.36	0.28	0.24	0.27	0.26	0.24	0.23	0.19	0.18	0.33	0.30
	PART	0.67	0.72	0.46	0.60	0.51	0.46	0.50	0.47	0.38	0.38	0.31	0.31	0.59	0.58
	UKIH	0.32	0.25	0.28	0.41	0.35	0.26	0.29	0.27	0.24	0.23	0.23	0.17	0.42	0.33
	FIXED	0.74	0.75	0.58	0.70	0.58	0.56	0.61	0.59	0.55	0.52	0.50	0.46	0.68	0.60
	LOCMIN	0.63	0.58	0.38	0.48	0.44	0.40	0.37	0.46	0.38	0.36	0.29	0.25	0.56	0.42
	SLIDE	0.74	0.73	0.53	0.68	0.58	0.55	0.61	0.60	0.49	0.46	0.46	0.40	0.66	0.60
	Geochemical	0.56	0.36	0.56	0.56	0.71	0.46	0.78	0.53	0.55	0.52	0.66	0.48	0.62	0.53

[a] Sites are Couturier (CO), Petite Savane (PS), Fourchette upstream (FU), Fourchette downstream (FD), Brûlée (BU), Noire (NO), Pot-au-Beurre (PB), Bellevue (BE), Ewing (EW), Aux Castors (CA), Branche 6 (BR6), Branche 21 (BR21), Cass (CS), and Brook (BO).

and significantly different from the actual quick flow conditions in these small agricultural watersheds. Because a subwatershed's drainage system influences the concentration time, these subwatersheds are drained quickly during rainfall events, with a very fast response within several hours.

PART set a long and flat recession after an event, extending over a period equal to or greater than N (eq. 1). The recession decreased gradually and followed a daily decline in the log of streamflow, which is the 0.1 log cycle per day usually associated with natural groundwater flow. Thus, the slow flow contribution was generally standardized and reflected more the lower section of the slow flow hydrographs compared to the geochemical method; the flashier upper section, largely of tile soil drainage, was excluded. This also reflected the differences in storage release processes. Very different behavior for tile release and groundwater flow can be deduced, as shown by the early and late segments of the slow flow recession curve from the geochemical method.

BFLOW's slow flow was characterized by low and smooth hydrographs. It was clear that the flashy hydrological behavior of the watersheds, associated with the drainage system, was misinterpreted by the method. The BFLOW method removed large-amplitude flows, regardless of their source, and thus filtered a significant contribution of quick flow to each increase in streamflow. Compared to the geochemical method, BFLOW considered a strong contribution from slow flow, mainly from tiles, as quick flow.

The scatter plots in figure A2 in the Appendix illustrate the comparisons between the estimated slow flow components from the non-calibrated filters and geochemical separation for the overall hydrograph analyses. Given the watershed landscape (spatial) characteristics, the non-calibrated filters tended to estimate higher slow flow fractions in the steep or hilly terrains of Appalachian (Madawaska and Tomifobia) and Laurentian (Champlain) landscapes, as compared to the St-Lawrence lowlands (Missisquoi, Esturgeon, and Lavallière). More scattered values showed these noticeable differences between these areas. The significant differences between the non-calibrated filters and the geochemical method are further detailed in the following section.

Statistical Analysis

The type 3 F-test for model effects showed significant interaction terms ($p < 0.05$) in relation to the slow flow (monthly average) response variable (table 8). In fact, there were significant interaction effects ($p < 0.0001$) from the method with year (2010 and 2011), the method with season (spring, summer, and fall), and the method with watershed relief (hilly and flat). The interaction of the method with subwatershed status (upstream and downstream) was considered to be only moderately significant ($p = 0.0083$). On the other hand, the type 3 F-test revealed a relatively significant interaction effect of the watershed relief with subwatershed status ($p = 0.0048$). This may be explained by the simultaneous location of upstream or downstream subwatersheds in both types of relief.

According to the significant interactions involving the methods, the least squares means (LS-means) are represented with bar plots in figure 4, where LS-means with the same letter are not significantly different. For the 14 experimental subwatersheds, significant effects of method with year were detected, with higher estimates of slow flow response in 2011, as shown in figure 4a, while the slow flow response was less important in 2010. As previously mentioned, 2011 was wetter than 2010, with significant increases in total water depth discharged at the subwatershed outlets.

Table 8. Type 3 tests of fixed effects.

	Degrees of Freedom			
Effect	Numerator	Denominator	F-Value	Pr > F
Relief	1	1128	0.90	0.3861
Status	1	1128	1.24	0.2661
Year	1	1128	17.89	<0.0001
Season	2	1128	46.98	<0.0001
Method	6	1128	113.45	<0.0001
Relief × Status	1	1128	8.00	0.0048
Relief × Year	1	1128	1.27	0.2595
Status × Year	1	1128	0.00	0.9933
Relief × Season	2	1128	0.34	0.7113
Status × Season	2	1128	0.08	0.9242
Season × Year	2	1128	0.56	0.5686
Relief × Method	6	1128	4.76	<0.0001
Status × Method	6	1128	2.90	0.0083
Year × Method	6	1128	5.74	<0.0001
Season × Method	12	1128	7.17	<0.0001

Figure 4a indicates that no filter estimates matched the geochemical method in 2010. There were similarities between the FIXED and PART estimates as well as between PART and SLIDE. In 2011, the FIXED and SLIDE estimates were not significantly different from the geochemical estimates, and PART was distinct from FIXED and SLIDE. LOCMIN, UKIH and BFLOW had the lowest estimates consecutively over the two years.

Figure 4b highlights the seasonality of the slow flow response. Spring estimates of slow flows were the highest, followed by fall estimates, due to high runoff during the snowmelt period and high-intensity fall precipitation. In addition, FIXED, SLIDE, and PART overestimated the slow flow response in spring compared to geochemical. The spring FIXED was classified as the highest, but it was not significantly different from the spring SLIDE. During this season, SLIDE was not different from geochemical and PART. Similarities between UKIH and BFLOW were also noted. However, in summer, geochemical predominated, followed by the pair of FIXED and SLIDE. The fall ranking is quite similar to the summer ranking. The fall geochemical estimates were not significantly different from those of spring compared to other methods. The similarities between FIXED and SLIDE, and between SLIDE and PART, were again highlighted.

Based on the watershed relief, the method estimates were significantly different from flat to hilly relief, as shown in figure 4c. This trend can be attributed to the higher rate of artificial drainage in lowland (flat) areas than in hilly relief. Figure 4c shows that the slow flow responses from the methods were significantly lower in lowlands than in hilly landscapes, as illustrated by the scatter plots in figure A2. There was no corresponding method for geochemical in lowlands. In addition, the FIXED and SLIDE estimates were significantly different, while the SLIDE estimates did not differ from those of PART. In hilly relief, there was no significant difference between geochemical, FIXED, and SLIDE, and FIXED was not significantly different from PART.

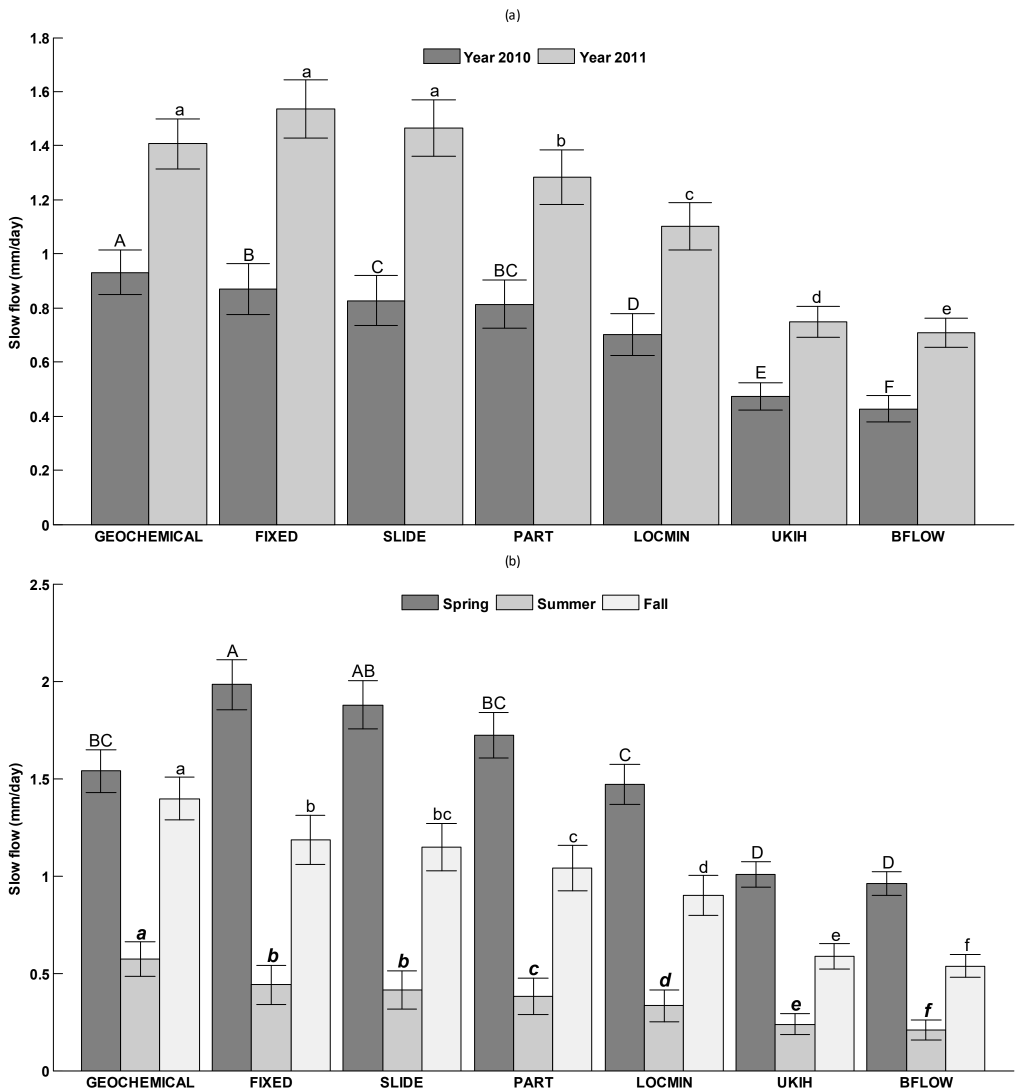

Figure 4. Least square means (LS-means) and differences between non-calibrated filters and geochemical method for estimating slow flow with respect to (a) years 2010 and 2011 and (b) seasons (spring, summer, and fall). Monthly average daily slow flow is presented in mm d^{-1}. All error bars represent one standard error of the mean. LS-means with the same letter are not significantly different at α = 0.05 with the Tukey-Kramer method for multiple pairwise comparisons.

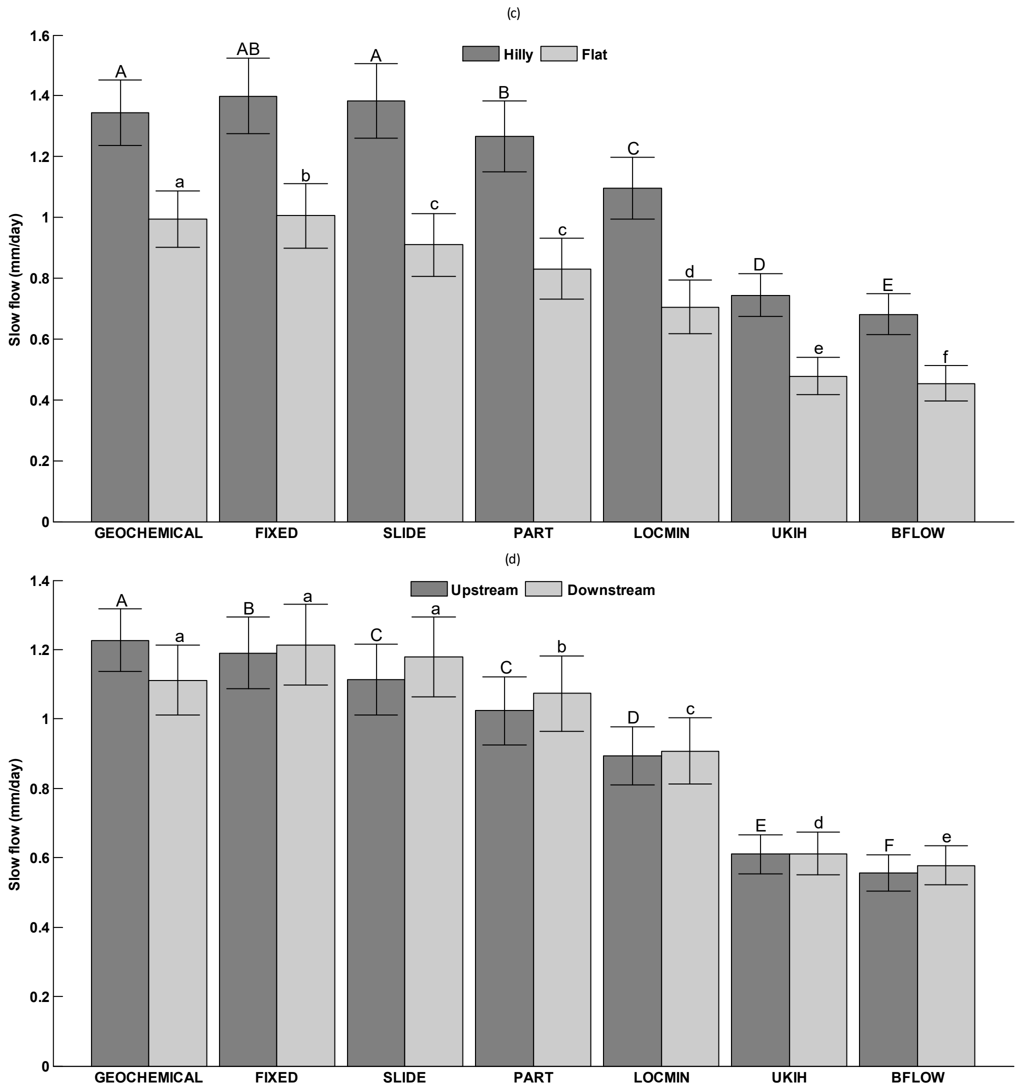

Figure 4 (continued). Least square means (LS-means) and differences between non-calibrated filters and geochemical method for estimating slow flow with respect to (c) watershed relief (hilly and flat) and (d) subwatershed status (upstream and downstream). Monthly average daily slow flow is presented in mm d^{-1}. All error bars represent one standard error of the mean. LS-means with the same letter are not significantly different at $\alpha = 0.05$ with the Tukey-Kramer method for multiple pairwise comparisons.

LOCMIN, UKIH, and BFLOW always provided the lowest estimates of slow flow.

The grouping by subwatershed status generally did not reveal any significant difference in method estimates between the upstream and downstream subwatersheds, as shown in figure 4d. The geochemical method showed a slight increase in slow flows in the upstream subwatersheds. In contrast, the filter methods associated this increase with the downstream subwatersheds, except for UKIH, which estimated a very similar response for both subwatersheds. According to the Tukey-Kramer method, the classification level of the non-calibrated filters increased in the downstream subwatersheds and was associated with the limited agricultural management practices. FIXED and SLIDE were always the most efficient and matched geochemical. The classification level of the non-calibrated filters on the downstream subwatersheds was generally quite similar to that of previous analyses, i.e., on hilly relief watersheds, in the spring season and in the year 2011. The methods adopted almost the same performance behavior. The effective performance of the non-calibrated filters could certainly be attributed to similar hydrological conditions in the mentioned cases. They particularly reflected conditions where the slow flow contribution to streamflow was presumed to be lower, while there was a significant contribution from quick flow. The relationship between the spring season and heavy precipitation may be due to soil moisture level, which easily reaches saturation in both cases, and surface runoff is expected to be predominant.

Similar conclusions could be drawn from the opposite cases: upstream watersheds, flat landscapes, fall and summer seasons, and the year 2010. Here, no filter method matched the geochemical method. The summer/fall and 2010 concordances were generally attributed to hydrological processes that predisposed more flow to slower pathways (tiles). Infiltration into the soil would depend on the higher variability in soil moisture during summer and fall than during spring. Practically, the increase in artificial drainage (in flat landscapes) and agricultural management practices (in upstream subwatersheds) point toward increased slow flow contributions. Beyond this, the heterogeneity of hydrological processes through the seasons lead to more complex hydrology, thereby affecting filter performance.

Based on the interpretation of the effects (of year, season, relief, and agricultural management practices) on the methods used for slow flow estimates, the performance of filters must be interpreted separately for each of these factors.

ECKHARDT FILTER CALIBRATION

Calibration Assuming Identical Aquifer Conditions for Twin Subwatersheds

In general, the daily slow flow calibration was satisfactory (table 9). PBIAS for calibration showed a positive low deviation between the slow flow values of the geochemical method and the Eckhardt filter. In addition, the NSE coefficients for slow flow calibration were good at most sites. The lower NSE coefficient for calibration on Fourchette upstream (0.40) and Ewing (0.39) showed that the filter overestimated peaks despite a PBIAS of almost zero for both subwatersheds. On the other hand, assuming identical aquifer conditions for upstream and downstream, the NSE coefficients for validation (downstream) were considerably worse than those for calibration (upstream), with values around zero and others negative.

The PBIAS values for validation indicated that the simulated slow flows were overestimated, thus significantly reducing the quick flow at the respective sites. As an example, the Noire site had one of the lowest statistical validation values (e.g., PBIAS of -63%). This was related to a higher contribution of quick flow on Noire (downstream) than on Brûlée (upstream). Similarly, at other sites with negative PBIAS, the same scenario was observed. Except on Fourchette (downstream) and in Baie Missisquoi (Aux Castors), the results were good over the validation period. The low NSE in calibration referred to the high runoff observed at Ewing compared to Aux Castors, even though they have relatively similar landscapes and land use. On both Fourchette subwatersheds, the geochemical method had already indicated similar hydrological responses. For the remaining subwatersheds, the results highlight very dissimilar hydrological responses between upstream and downstream sites. The downstream subwatersheds were more susceptible to high surface runoff than the upstream subwatersheds. Therefore, no parameter could be transferred from upstream to downstream. Obviously, each subwatershed was unique, indicating that BFI_{max} was limited to a given site.

Calibration Based on Individual Subwatershed Hydrological Response

The calibration statistics in table 10 indicate good adjustment of the daily slow flows. Only Petite Savane showed an overestimation of 20% (PBIAS) of slow flows over the calibration period, despite an RMSE of 0.94 and NSE of 0.52. This overestimation occurred in spring and fall of 2010. The Ewing calibration over 2007 to 2009 also yielded an NSE of -0.45. After a considerable overestimation of the 2008 spring runoff, the peaks simulations were definitely affected, reducing the NSE significantly. On the adjacent Aux Castors site, overestimates of spring runoff in 2008 and heavy rainfall in June 2006 did not significantly lower the NSE (of 0.44). It was assumed here that the training of the BFI_{max} parameter on data from more periods of calibration (2005 to 2009) may have contributed to a better NSE at Aux Castors than at Ewing. In the validation, most sites had lower NSE than in the calibration. Slow flow contributions were overestimated, as indicated by the PBIAS.

The differences between calibration and validation statistics highlighted two main points. First, the hydrological conditions were very different between the calibration and validation periods. The validation period (2011) was associated with high snow cover, followed by snowmelt conditions leading to more intense quick runoff in the spring, and heavy precipitation in the summer and fall. Consequently, filter adjustment during the validation period was particularly low in subwatersheds where landscape conditions were more vulnerable to quick runoff, such as Petite Savane (NSE = -3.12; PBIAS = -0.68), Brook (NSE = 0.30; PBIAS = -0.29), and Noire (NSE = 0.20; PBIAS = -0.25). The filter largely overestimated the slow flow values, resulting in poor NSE and negative PBIAS.

Second, the Eckhardt filter simulations showed a dependence on calibration data. The BFI_{max} estimates (table 11) represented hydrological conditions that approximated typical slow flow ratios derived from the calibration data. The validation simulations were therefore highly biased by the calibration results, resulting in poor statistics. For example, on Ewing, by changing the calibration period of 2007 to 2009 for the period of 2010 to 2011, instead of having a BFI_{max} of 0.75, a new BFI_{max} of 0.58 was obtained. This demonstrated how the estimates of BFI_{max} can be different when using different calibration data. There is a substantial difference between BFI_{max} of 0.58 in a wet year and a BFI_{max} of 0.75 in a dry or normal year. Wet and dry years would give different estimates of BFI_{max}, as would a wet period with frequent runoff events compared to a moderate or dry period dominated

Table 9. Model fit statistics of calibration using upstream subwatersheds and validation using downstream subwatersheds.[a]

	Calibration				Validation[b]			
Watershed	Subwatershed	RMSE	NSE	PBIAS	Subwatershed	RMSE	NSE	PBIAS
Madawaska	CO	0.74	0.82	0.00	PS	1.29	0.02	-0.23*
Fourchette	FU	1.08	0.40	0.01	FD	0.78	0.71	0.01
Champlain	BU	0.91	0.87	0.02	NO	1.20	-0.55**	-0.63*
Baie Lavallière	PB	0.56	0.82	0.01	BE	1.04	0.11	-0.33*
Baie Missisquoi	EW	0.82	0.39	0.00	CA	0.78	0.59	-0.03
Esturgeon	BR6	0.22	0.90	0.00	BR21	1.40	-0.63**	-0.24*
Tomifobia	CS	0.91	0.74	0.00	BO	1.51	0.06	-0.19*

[a] Sites are Couturier (CO), Fourchette upstream (FU), Brûlée (BU), Pot-au-Beurre (PB), Ewing (EW), Branche 6 (BR6), Cass (CS), Petite Savane (PS), Fourchette downstream (FD), Noire (NO), Bellevue (BE), Aux Castors (CA), Branche 21 (BR21), and Brook (BO).

[b] Asterisks indicate (**) negative NSE values and (*) values outside -10% ≤ PBIAS ≤ 10%.

Table 10. Model fit statistics of calibration and validation at each site.

Watershed	Subwatershed[a]	Calibration[b] RMSE	Calibration[b] NSE	Calibration[b] PBIAS	Validation[b] RMSE	Validation[b] NSE	Validation[b] PBIAS
Madawaska	CO	0.71	0.83	0.00	0.89	0.71	-0.11*
	PS	0.94	0.52	-0.21*	2.13	-3.12**	-0.68*
Fourchette	FU	1.08	0.40	0.01	1.14	0.48	-0.05
	FD	0.80	0.70	0.00	0.71	0.71	-0.04
Champlain	BU	0.65	0.90	0.02	1.57	0.65	-0.30*
	NO	0.32	0.88	-0.03	0.87	0.20	-0.25*
Baie Lavallière	PB	0.44	0.86	0.01	0.89	0.50	-0.19*
	BE	0.54	0.68	0.01	0.84	0.41	-0.16*
Baie Missisquoi	EW	0.89	-0.45**	0.00	0.93	-15.9**	0.00
	CA	0.71	0.44	0.00	0.95	-22.4**	0.25*
Esturgeon	BR6	0.24	0.89	0.00	0.29	0.74	-0.18*
	BR21	0.96	0.23	0.00	1.27	-0.49**	-0.26*
Tomifobia	CS	0.73	0.66	0.00	1.54	0.54	-0.24*
	BO	1.22	0.16	-0.02	1.52	0.30	-0.29*

[a] Sites are Couturier (CO), Petite Savane (PS), Fourchette upstream (FU), Fourchette downstream (FD), Brûlée (BU), Noire (NO), Pot-au-Beurre (PB), Bellevue (BE), Ewing (EW), Aux Castors (CA), Branche 6 (BR6), Branche 21 (BR21), Cass (CS), and Brook (BO).

[b] Asterisks indicate (**) negative NSE values and (*) values outside -10% ≤ PBIAS ≤ 10%.

by slow flow. BFI_{max} calibrated for a wetter (or moderate or dry) climate than the validation climate may lead to underestimation (or overestimation) of the slow flow. The periods 2005, 2006, and 2011 could be one such example; the contribution of slow flow was less significant than in other years, as indicated earlier in table 5.

The estimates of BFI_{max} in table 11 varied from site to site and were all greater than 0.50. The values were generally higher at upstream subwatersheds, corresponding to slow flow dominated sites, thus reflecting the information provided by the geochemical method. The applied values of the recession parameter (a) are also shown in table 11. The values of a for slow flow were generally small due to the uniform representation of the recession slopes of slow flows, having both steeper and smoother segments.

Comparison of Calibrated Eckhardt Filter to Geochemical Method

In general, the slow flow estimates of the Eckhardt filter were quite close to the 1:1 line on the scatter plots with geochemical estimates (fig. 5). The scatter plots showed that larger errors were associated with higher flow values. This overestimation seemed to be more pronounced during periods of high discharge. Table A1 in the Appendix provides detailed performance measures during the three seasons. This table shows that the Eckhardt filter estimates were highly correlated with the geochemical estimates at all sites according to correlation coefficient (R) values. Comparing the filter performance between seasons, downstream subwatersheds had a higher overestimation in spring 2010, while there was also an underestimation of slow flow in summer and fall. Spring 2011 had the lowest performances at all

Table 11. Eckhardt filter parameters at each site.[a]

Parameter	Madawaska CO	Madawaska PS	Fourchette FU	Fourchette FD	Champlain BU	Champlain NO	Baie Lavallière PB	Baie Lavallière BE	Baie Missisquoi EW	Baie Missisquoi CA	Esturgeon BR6	Esturgeon BR21	Tomifobia CS	Tomifobia BO
a	0.125	0.171	0.128	0.174	0.110	0.257	0.121	0.167	0.131	0.238	0.195	0.147	0.129	0.170
BFI_{max}	0.65	0.68	0.73	0.73	0.84	0.53	0.86	0.70	0.75	0.67	0.75	0.64	0.82	0.70

[a] Sites are Couturier (CO), Petite Savane (PS), Fourchette upstream (FU), Fourchette downstream (FD), Brûlée (BU), Noire (NO), Pot-au-Beurre (PB), Bellevue (BE), Ewing (EW), Aux Castors (CA), Branche 6 (BR6), Branche 21 (BR21), Cass (CS), and Brook (BO).

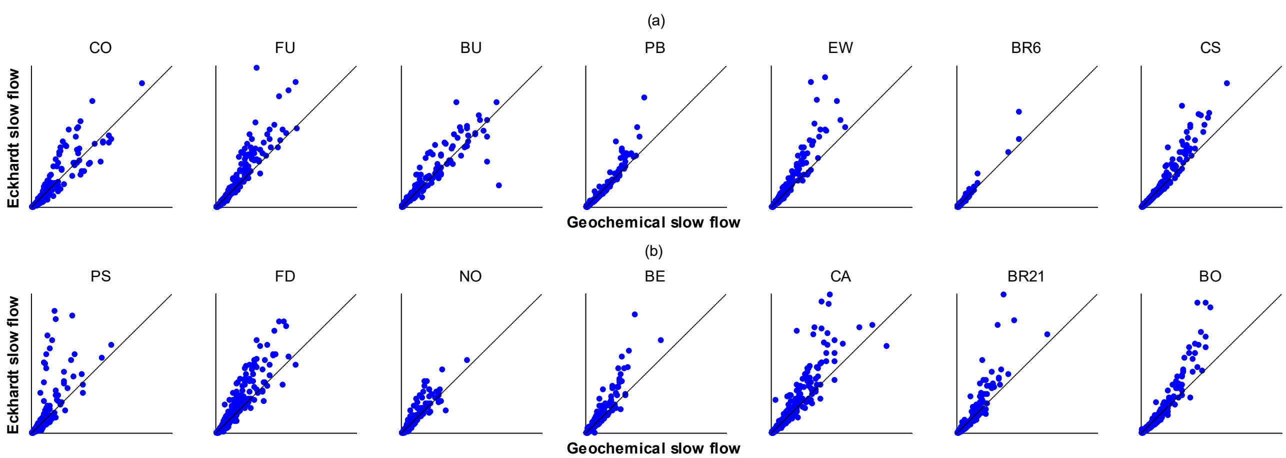

Figure 5. Comparisons of daily slow flow estimates (mm d[-1]) from calibrated Eckhardt filter and geochemical method for (a) upstream and (b) downstream sites. Sites are Couturier (CO), Fourchette upstream (FU), Brûlée (BU), Pot-au-Beurre (PB), Ewing (EW), Branche 6 (BR6), Cass (CS), Petite Savane (PS), Fourchette downstream (FD), Noire (NO), Bellevue (BE), Aux Castors (CA), Branche 21 (BR21), and Brook (BO).

sites, with poor NSE, while PBIAS showed overestimation of slow flow at almost all sites. In summer and fall, NSE improved but PBIAS was still negative.

For comparison, daily slow flow hydrographs from the Eckhardt filter and geochemical method are presented in figure 6 for the Aux Castors subwatershed in 2010 and 2011. The slow flow estimates of the filter have been excessively elevated during the relevant seasons of spring and fall.

The Eckhardt filter hydrographs for slow flow appeared to approximate more closely to the total flow trends, so that the peaks of slow flow were overestimated. The hydrograph separation of the Eckhardt filter is mainly based on the predetermined BFI_{max} parameter. At higher BFI_{max} conditions, slow flows were dominant, while quick flows were less significant. We know that snowmelt is significant in the spring and that the precipitation during this period is sometimes similar to that in summer, but it generates much higher surface runoff (about 40% on average of the total annual water yield). In fact, the hydrological response is more dependent on waterlogged soils than simply on precipitation depth and intensity. Thus, saturation-excess runoff predominates in the spring, while infiltration-excess runoff most likely prevails for high-intensity rainfall events in the summer. When analyzing the spring runoff period and the recurrence of extreme events such as high-intensity precipitation, the filter did not simulate any significant changes in the slow flow response. This is shown in figures A3 and A4 in the Appendix, which compare the daily fractions of slow flow from the Eckhardt filter and geochemical method for the periods 2010 and 2011.

The linear concept of the Eckhardt filter yields no information on slow flow response behavior that could be useful in capturing seasonal variation. As shown in figures A3 and A4, the BFI_{max} parameter, used as a slow response index, simply limited the filter results to a regular ratio of slow flow in the stream. This is consistent with the observation by Nathan and McMahon (1990), who analyzed the baseflow hydrographs of a smoothed minima technique (Institute of Hydrology, 1980) and a recursive digital filter (Lyne and Hollick, 1979). They noted that the methods did not attempt to simulate baseflow conditions; instead, the filter was aimed at deriving an objective index related to baseflow. To explain the dynamics of the relationship between slow flow and streamflow, the geochemical results reflected a strong seasonal dependence (figs. A3 and A4). This is strongly related to the temporal variability of soil moisture. Accordingly, the low ratios of slow flow to streamflow were related to snowmelt and rainfall events, when soil moisture reaches saturation faster. Furthermore, comparing the years 2010 and 2011, the climatic conditions with heavy and frequent rainfalls in 2011 that were outside of seasonality modulated the flow generation mechanisms, and thus the corresponding slow flow ratios often varied from high to low. This was particularly pronounced in the downstream subwatersheds, which were more affected by surface runoff. In general, between events, slow flow ratios were at their highest.

DISCUSSION

GEOCHEMICAL METHOD LIMITATIONS

Quick Flow Conductivity (C_q) Remains Constant and Refers to the Lowest Streamflow Conductivity Value

The estimation of quick flow conductivity (C_q) was approximated by assimilating it to the lowest stream water conductivity. The quick flow conductivity was relatively constant at the outlet and represented 100% quick flow conditions. The lowest conductivity value observed during the highest flows was apparently a reliable measure of quick flow conductivity, as it indicated the least charged inflow to

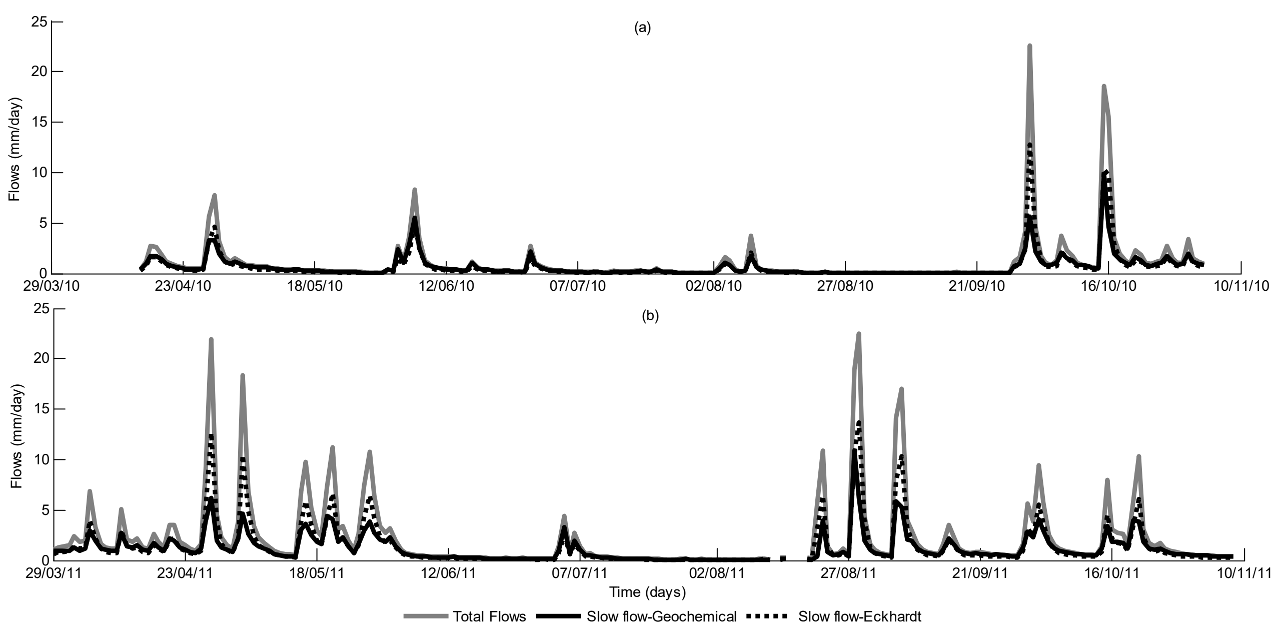

Figure 6. Comparison of daily slow flow separation from total flow using geochemical method and Eckhardt filter for Aux Castors subwatershed in (a) 2010 and (b) 2011.

the stream. This value represented the weighted average conductivity of all surface runoff inputs occurring upstream of the outlet. Because conductivity values are influenced by the duration and intensity of a hydrologic event, it is clear that runoff also influences the duration of low conductivity values. Considering that a portion of the streamflow may be slow, even at the highest flows, this assumption may underestimate the slow flow during extremely high flow events, when the streamflow conductivities are close to the selected minimum (C_q) value. It should be noted that the minimum values observed were limited to current databases. If new measurements are added, it is necessary to ensure that the selected values remain the lowest recorded over the total observations. Indeed, selected values could change, given the large temporal variability of hydrological conditions.

Slow Flow Conductivity (C_s) Remains Constant and Refers to the Pre-Event Streamflow Conductivity Values

It was reasonable to use the pre-event conductivity values to estimate C_s, as there was practically no quick flow for seven consecutive days without rain. The C_s was limited to a constant throughout the hydrograph separation process. Uncertainty may arise when the conductivity of the total flow cannot reach the maximum (assumed to be 100% slow flow) before a future event, and the contribution of the slow flow may be underestimated. This would lead to substantial concerns about the correct value of C_s during a given event or season. Assuming that C_s variations occur at each event would get C_s values closer to the streamflow values, resulting in higher slow flow contributions. The latter could be considered to include a portion of quick flow in case a low contribution of slow flow is observed. This procedure would require more user experience and more elaborate manipulation to determine event-specific conductivity values. The use of a constant C_s value was a simple approach for the application of the geochemical method and for processing long-term data records.

Filtering Approach Limitations

Based on the assumptions of the non-calibrated filters, the quick runoff duration (FIXED, SLIDE, LOCMIN, PART), the high amplitude of the quick flow (BFLOW), and the low minimum flow conditions (UKIH, FIXED, SLIDE, LOCMIN) used to characterize slow flow hydrographs all focused on quick runoff as a prominent process in the watershed. Therefore, slow flow was of minor significance. One of our conclusions from the MANOVA model highlighted this fact. The analysis showed that the performance of the filters increased for conditions dominated by the contribution of quick flow to the stream, such as during the snowmelt period (spring), during heavy precipitation, and in subwatersheds characterized by landscape conditions more vulnerable to quick runoff. On the other hand, the filter performance decreased as the slow flow contribution increased, in summer and fall, and in lowland landscapes, which are generally associated with higher rates of tile drainage than in hilly and steep relief.

Quick runoff to agricultural streams resulting from changes in the natural drainage status of agricultural watersheds is defined by the surface runoff-infiltration relationship, which is substantially altered. Greater infiltration sustains higher slow flow and low minimum flows into agricultural streams (Schilling and Libra, 2003). The routing of water according to the soil or landscape properties is manipulated to facilitate efficient use of the drainage system. Thus, water storage and the duration of both surface and subsurface runoff are shortened. Under these conditions, using the above assumptions, and relying only on the streamflow values, it is impossible to differentiate between the different sources of hydrograph fluctuations. Therefore, both slow flow and quick flow are misinterpreted, with slow flow identified as quick flow, or vice versa. This supports the observation of Raffensperger et al. (2017) regarding diverse hydrological components (such as interflow, macropore flow, etc.) and human modifications (such as artificial drainage): the limitations resulting from the assumptions of existing hydrograph separation methods may be evidence of poor results in describing hydrological system responses.

Some studies (Stewart et al., 2007; Vasconcelos et al., 2013) have suggested calibrating the N parameter of the empirical equation (eq. 1) to achieve the best possible approximation of slow flow. This would not be recommended for small watersheds with fast hydrological response, where various processes are involved in runoff generation. Otherwise, the physical characteristics of the watersheds would be excluded without being fully investigated. The calculation of quick runoff duration based on equation 1 cannot be applied because the quick runoff duration and cessation are a function of more than just the contributing drainage area. Any new filtering approach should consider one or more factors that influence the temporal scale of watershed runoff.

Typically, filtering methods are limited to quick flow in the drainage area and slow flow entering the stream through delayed pathways consisting of a single outflow from groundwater (primarily water flowing from a shallow aquifer). Based on this approach, subsurface flows are not relevant. The particular characterization of slow flow hydrographs by analysis of the exponential behavior of recession curves (PART) generally reflects the conceptual behavior of groundwater discharge. This representation of slow flow in agricultural streams resulted in a lower component as slow flow. The filter calculations resulted in a significant portion of slow flow expected from tile drains as quick flow. Flow through the tiles is a complex process that requires different approaches. It is evident that in faster conditions (routing and residence time), flow through the tiles is a physical process distinct from that of water which, under natural conditions (delayed routing and residence time), infiltrates directly into the soil and flows into stream or contributes to aquifer recharge and discharge.

Similarly, the assumption of linear aquifer outflow that simulates the slow Eckhardt filter component of the hydrograph is a simplified assumption for groundwater release. Slow flow is linearly proportional to the available water ratio in storage, as set by BFI_{max}. Describing the non-linear evolution of the system over time is not possible. Although the filter was adjusted with good statistical performance measures, the BFI_{max} parameter was simply a value calibrated to specific instantaneous values of slow flow and represented the average slow flow conditions at a specific period of time. This value varied significantly depending on the data used for calibration. When conditions shifted beyond the range of prior calibration conditions, the filter performed poorly, for example, when tested with validation data with different rainfall characteristics. In this way, the filter did not extrapolate well, as the filter approach is inconsistent with the fundamental mechanisms underlying hydrological processes. Thus, the filter became unreliable. In cases like this, as long as the underlying premises of the filter do not correspond to physical reality, the filter may perform well enough on calibrated sections, but its long-term stability remains uncertain. Therefore, there is a need for hydrograph separation methods that are better informed by hydrological insight, as demonstrated by the geochemical method in characterizing the streamflow components.

The increasing complexity of agricultural watersheds in relation to artificial drainage, agriculture management practices, the heterogeneity of hydrological processes, and varying rainfall patterns is expected to result in a more complex slow flow response. Simplifications of filter assumptions are therefore less likely to provide effective estimates of slow flow. For filter-based hydrograph separation, there is still much to learn about agricultural watersheds. An investigation of the characterization of soil-shallow aquifer storage dynamics and a description of the relationship between surface runoff and infiltration would improve our understanding of streamflow generation processes, which would enhance the hydrograph separation concepts for such watersheds.

CONCLUSIONS

In this study, the geochemical method strongly contributed to the evaluation of automated filter methods. The use of geochemical data for different years provided information to characterize hydrological responses and their components, which has become a priority in the validation of filter methods. The monthly estimates used to assess the performance of the methods with respect to the various factors influencing slow flow showed that, under particular conditions, some filters were able to capture the average slow flow comparable to that estimated by the geochemical method. This suggests that caution should be taken in the application of these methods, depending on the flow dynamics of the watershed under study, in relation to the relevant factors influencing the routing of water. Improved routing of water through artificial drainage and agricultural management practices resulted in substantial hydrological modifications. The basic concepts of filters are simple procedures for such challenging hydrology. The relatively higher variation in daily observations (based on the geochemical method) showed that it is essential to accurately capture slow flow behavior at finer timescales. Given the high heterogeneity of hydrological processes, the routine application of basic filter concepts is not sufficient to address the variable nature of the hydrological response. The variability scale of geochemical separation, i.e., regional (agro-climatic) and local (twin subwatersheds), proved that adequate separation is always relevant. However, the validation of filters without a tracer is very limited and almost unsuitable for these agricultural watersheds.

Further work should explore the automatic calibration of hydrological models for hydrograph separation. This in-depth tracer-based understanding will be used for the application and validation. Although our evaluation is limited to agricultural watersheds in Québec, the key findings of this study should be applicable over a wide range of hydrological environments.

ACKNOWLEDGEMENTS

The authors gratefully acknowledge the reviewers' comments, which greatly improved the manuscript. We thank Andrew R. Piggott (Piggott et al., 2005) for providing the computer codes for the FIXED, LOCMIN, SLIDE, PART, and UKIH filters. We also thank Gaétan Daigle for assistance with the statistical analysis with MANOVA. The first author acknowledges financial and data support from IRDA (Institut de Recherche et de Développement en Agroenvironnement).

REFERENCES

Arnold, J. G., & Allen, P. M. (1999). Automated methods for estimating baseflow and groundwater recharge from streamflow records. *JAWRA, 35*(2), 411-424. https://doi.org/10.1111/j.1752-1688.1999.tb03599.x

Arnold, J. G., Allen, P. M., Muttiah, R., & Bernhardt, G. (1995). Automated base flow separation and recession analysis techniques. *Groundwater, 33*(6), 1010-1018. https://doi.org/10.1111/j.1745-6584.1995.tb00046.x

Beaudin, I., Deslandes, J., Michaud, A. R., Bonn, F., & Madramootoo, C. A. (2006). Variabilité spatio-temporelle des exportations de sédiments et de phosphore dans le bassin versant de la Rivière aux Brochets au sud-ouest du Québec: Partie I – Paramètrage, calibrage et validation du modèle SWAT. *Agrosol. 17*(1), 4-20.

Beaulieu, R. (2001). Historique des travaux de drainage au Québec et état du réseau hydrographique. Québec City, QC, Canada: Bureau d'audiences publiques sur l'environnement (BAPE). Retrieved from http://142.44.245.8/sections/mandats/prod-porcine/documents/Bio115.pdf

Blann, K. L., Anderson, J. L., Sands, G. R., & Vondracek, B. (2009). Effects of agricultural drainage on aquatic ecosystems: A review. *Crit. Rev. Environ. Sci. Tech., 39*(11), 909-1001. https://doi.org/10.1080/10643380801977966

Brodie, R. S., & Hostetler, S. (2005). A review of techniques for analysing base-flow from stream hydrographs. *Proc. NZHS-IAH-NZSSS Conf.*

Chapman, T. (1999). A comparison of algorithms for streamflow recession and baseflow separation. *Hydrol. Proc., 13*(5), 701-714. https://doi.org/10.1002/(sici)1099-1085(19990415)13:5<701::aid-hyp774>3.0.co;2-2

Chapman, T. G. (1991). Comment on "Evaluation of automated techniques for base flow and recession analyses" by R. J. Nathan and T. A. McMahon. *Water Resour. Res., 27*(7), 1783-1784. https://doi.org/10.1029/91wr01007

Chapman, T. G., & Maxwell, A. I. (1996). Baseflow separation: Comparison of numerical methods with tracer experiments. *Proc. 23rd Hydrology and Water Resourcces Symp.* (pp. 539-545). Barton, ACT, Australia: Institution of Engineers.

Coron, L., Andréassian, V., Perrin, C., Lerat, J., Vaze, J., Bourqui, M., & Hendrickx, F. (2012). Crash testing hydrological models in contrasted climate conditions: An experiment on 216 Australian catchments. *Water Resour. Res., 48*(5), W05552. https://doi.org/10.1029/2011wr011721

Deslandes, J., Beaudin, I., Michaud, A., Bonn, F., & Madramootoo, C. A. (2007). Influence of landscape and cropping system on phosphorus mobility within the Pike River watershed of southwestern Québec: Model parameterization and validation. *Canadian Water Resour. J., 32*(1), 21-42. https://doi.org/10.4296/cwrj3201021

Duan, Q. Y., Gupta, V. K., & Sorooshian, S. (1993). Shuffled complex evolution approach for effective and efficient global minimization. *J. Optim. Theory Appl., 76*(3), 501-521. https://doi.org/10.1007/BF00939380

Eckhardt, K. (2005). How to construct recursive digital filters for baseflow separation. *Hydrol. Proc., 19*(2), 507-515. https://doi.org/10.1002/hyp.5675

Eckhardt, K. (2008). A comparison of baseflow indices, which were calculated with seven different baseflow separation methods. *J. Hydrol., 352*(1), 168-173. https://doi.org/10.1016/j.jhydrol.2008.01.005

Enright, P., & Madramootoo, C. A. (2004). Phosphorus losses in surface runoff and subsurface drainage waters on two agricultural fields in Québec. ASABE Paper No. 701P0304. St. Joseph, MI: ASABE. https://doi.org/10.13031/2013.15722

Fraser, H., & Fleming, R. (2001). Environmental benefits of tile drainage: Literature review. Prepared for Land Improvement Contractors of Ontario. Guelph, ON, Canada: University of Guelph. Retrieved from https://www.ridgetownc.com/research/documents/fleming_drainage.pdf

Gonzales, A. L., Nonner, J., Heijkers, J., & Uhlenbrook, S. (2009). Comparison of different base flow separation methods in a lowland catchment. *Hydrol. Earth Syst. Sci., 6*(2). https://doi.org/10.5194/hess-13-2055-2009

Halford, K. J., & Mayer, G. C. (2000). Problems associated with estimating groundwater discharge and recharge from stream-discharge records. *Groundwater, 38*(3), 331-342. https://doi.org/10.1111/j.1745-6584.2000.tb00218.x

Hall, F. R. (1968). Base-flow recession: A review. *Water Resour. Res., 4*(5), 973-983. https://doi.org/10.1029/WR004i005p00973

Institute of Hydrology. (1980). Low flow studies Report No 1. Wallingford, UK: Institute of Hydrology.

Kronholm, S. C., & Capel, P. D. (2015). A comparison of high-resolution specific conductance-based end-member mixing analysis and a graphical method for baseflow separation of four streams in hydrologically challenging agricultural watersheds. *Hydrol. Proc., 29*(11), 2521-2533. https://doi.org/10.1002/hyp.10378

Linsley, R. K., Kohler, M. A., & Paulhus, J. L. (1982). *Hydrology for engineers* (3rd. ed.). New York, NY: McGraw-Hill.

Lyne, V., & Hollick, M. (1979). Stochastic time-variable rainfall-runoff modelling. *Proc. Institute of Engineers National Conf.* (pp. 89-93). Barton, ACT, Australia: Institution of Engineers.

Matsubayashi, U., Velasquez, G. T., & Takagi, F. (1993). Hydrograph separation and flow analysis by specific electrical conductance of water. *J. Hydrol., 152*(1), 179-199. https://doi.org/10.1016/0022-1694(93)90145-Y

Mau, D. P., & Winter, T. C. (1997). Estimating groundwater recharge from streamflow hydrographs for a small mountain watershed in a temperate humid climate, New Hampshire, USA. *Groundwater, 35*(2), 291-304. https://doi.org/10.1111/j.1745-6584.1997.tb00086.x

Michaud, A. R., Desjardins, J., Lauzier, R., & Grenier, M. (2009c). Suivi de la qualité de l'eau des bassins versants expérimentaux Ewing et Aux Castors. Québec City, QC, Canada: IRDA Québec. Retrieved from https://www.irda.qc.ca/fr/publications/suivi-de-la-qualite-de-l-eau-des-bassins-versants-experimentaux-ewing-et-aux-castors-dans-le-cadre-du-projet-lisiere-verte/

Michaud, A. R., Deslandes, J., Desjardins, J., & Grenier, M. (2009b). Réseau d'actions concertées en bassins versants agricoles. Québec City, QC, Canada: IRDA Québec. Retrieved from https://www.irda.qc.ca/fr/publications/reseau-d-actions-concertees-en-bassins-versants-agricoles/

Michaud, A. R., Poirier, S. C., Desjardins, J., Grenier, M., & Saint-Laurent, I. (2009a). Évaluation des exportations de surface et souterraines de phosphore en sol drainé. Québec City, QC, Canada: IRDA Québec. Retrieved from https://www.irda.qc.ca/assets/documents/Publications/documents/michaud-et-al-2009_rapport_exportations_p_sol_draine.pdf

Michaud, A. R., Poirier, S. C., Desjardins, J., Grenier, M., & Saint-Laurent, I. (2012). Observatoire de la qualité de l'eau de surface en bassins versants agricoles. Québec City, QC, Canada: IRDA Québec. Retrieved from https://www.irda.qc.ca/assets/documents/Publications/documents/michaud-et-al-2012_rapport_observatoire_periode_reference.pdf

Michaud, A. R., Poirier, S.-C., & Whalen, J. K. (2019). Tile drainage as a hydrologic pathway for phosphorus export from an agricultural subwatershed. *J. Environ. Qual., 48*(1), 64-72. https://doi.org/10.2134/jeq2018.03.0104

Moriasi, D. N., Arnold, J. G., Van Liew, M. W., Bingner, R. L., Harmel, R. D., & Veith, T. L. (2007). Model evaluation guidelines for systematic quantification of accuracy in watershed simulations. *Trans. ASABE, 50*(3), 885-900. https://doi.org/10.13031/2013.23153

Muma, M., Rousseau, A. N., & Gumiere, S. J. (2016). Assessment of the impact of subsurface agricultural drainage on soil water storage and flows of a small watershed. *Water, 8*(8), 326. https://doi.org/10.3390/w8080326

Nathan, R. J., & McMahon, T. A. (1990). Evaluation of automated techniques for base flow and recession analyses. *Water Resour. Res., 26*(7), 1465-1473. 10.1029/WR026i007p01465

Neff, B. P., Day, S. M., Piggott, A. R., & Fuller, L. M. (2005). Base flow in the Great Lakes basin. USGS Scientific Investigations Report 2005-5217. Reston, VA: U.S. Geological Survey. https://doi.org/10.3133/sir20055217

Partington, D., Brunner, P., Simmons, C. T., Werner, A. D., Therrien, R., Maier, H. R., & Dandy, G. C. (2012). Evaluation of outputs from automated baseflow separation methods against simulated baseflow from a physically based, surface water-groundwater flow model. *J. Hydrol., 458-459*, 28-39. https://doi.org/10.1016/j.jhydrol.2012.06.029

Pellerin, B. A., Wollheim, W. M., Feng, X., & Vörösmarty, C. J. (2008). The application of electrical conductivity as a tracer for hydrograph separation in urban catchments. *Hydrol. Proc., 22*(12), 1810-1818. https://doi.org/10.1002/hyp.6786

Pettyjohn, W. A., & Henning, R. (1979). Preliminary estimate of groundwater recharge rates, related streamflow and water quality in Ohio. Project Completion Report No 552. Columbus: Ohio State University, Water Resources Center.

Piggott, A. R., Moin, S., & Southam, C. (2005). A revised approach to the UKIH method for the calculation of baseflow. *Hydrol. Sci. J., 50*(5), 911-920. https://doi.org/10.1623/hysj.2005.50.5.911
Pilgrim, D. H., Huff, D. D., & Steele, T. D. (1979). Use of specific conductance and contact time relations for separating flow components in storm runoff. *Water Resour. Res., 15*(2), 329-339. https://doi.org/10.1029/WR015i002p00329
Pinder, G. F., & Jones, J. F. (1969). Determination of the groundwater component of peak discharge from the chemistry of total runoff. *Water Resour. Res., 5*(2), 438-445. https://doi.org/10.1029/WR005i002p00438
Poirier, S.-C., Whalen, J. K., & Michaud, A. R. (2012). Bioavailable phosphorus in fine-sized sediments transported from agricultural fields. *SSSA J., 76*(1), 258-267. https://doi.org/10.2136/sssaj2010.0441
Raffensperger, J. P., Baker, A. C., Blomquist, J. D., & Hopple, J. A. (2017). Optimal hydrograph separation using a recursive digital filter constrained by chemical mass balance, with application to selected Chesapeake Bay watersheds. Scientific Investigations Report 2017-5034. Reston, VA: U.S. Geological Survey. https://doi.org/10.3133/sir20175034
Rutledge, A. T. (1998). Computer programs for describing the recession of groundwater discharge and for estimating mean groundwater recharge and discharge from streamflow records: Update. USGS Water Resources Investigations Report 98-4148. Reston, VA: U.S. Geological Survey.
Rutledge, A. T. (2005). The appropriate use of the Rorabaugh model to estimate groundwater recharge. *Groundwater, 43*(3), 292-293. https://doi.org/10.1111/j.1745-6584.2005.0022.x
Santhi, C., Allen, P. M., Muttiah, R. S., Arnold, J. G., & Tuppad, P. (2008). Regional estimation of base flow for the conterminous United States by hydrologic landscape regions. *J. Hydrol., 351*(1), 139-153. https://doi.org/10.1016/j.jhydrol.2007.12.018
Schilling, K. E., & Helmers, M. (2008). Effects of subsurface drainage tiles on streamflow in Iowa agricultural watersheds: Exploratory hydrograph analysis. *Hydrol. Proc., 22*(23), 4497-4506. https://doi.org/10.1002/hyp.7052
Schilling, K. E., & Libra, R. D. (2003). Increased baseflow in Iowa over the second half of the 20th century. *JAWRA, 39*(4), 851-860. https://doi.org/10.1111/j.1752-1688.2003.tb04410.x
Schwartz, S. S. (2007). Automated algorithms for heuristic base-flow separation. *JAWRA, 43*(6), 1583-1594. https://doi.org/10.1111/j.1752-1688.2007.00130.x
Sloto, R. A., & Crouse, M. Y. (1996). HYSEP: A computer program for streamflow hydrograph separation and analysis. USGS Water Resources Investigations Report 96-4040. Reston, VA: U.S. Geological Survey.
Smith, E. A. (2012). Spatial and temporal variability of preferential flow in a subsurface-drained landscape in north-central Iowa. PhD diss. St. Paul, MN: University of Minnesota, Water Resources Science.
Smith, E. A., & Capel, P. D. (2018). Specific conductance as a tracer of preferential flow in a subsurface-drained field. *Vadose Zone J., 17*(1), 170206. https://doi.org/10.2136/vzj2017.11.0206
Stewart, M., Cimino, J., & Ross, M. (2007). Calibration of base flow separation methods with streamflow conductivity. *Groundwater, 45*(1), 17-27. https://doi.org/10.1111/j.1745-6584.2006.00263.x
Stoelzle, M., Schuetz, T., Weiler, M., Stahl, K., & Tallaksen, L. M. (2019). Beyond binary baseflow separation: A delayed-flow index for multiple streamflow contributions. *Hydrol. Earth Syst. Sci., 24*(2), 849-867. https://doi.org/10.5194/hess-24-849-2020
Thomas, B. F., Vogel, R. M., & Famiglietti, J. S. (2015). Objective hydrograph baseflow recession analysis. *J. Hydrol., 525*, 102-112. https://doi.org/10.1016/j.jhydrol.2015.03.028
Vasconcelos, V. V., Junior., M., Pereira, P., & Hadad, R. M. (2013). Estimation of flow components by recursive filters: Case study of Paracatu River basin (SF-7), Brazil. *Geologia USP, Série Científica, 13*, 3-24. https://doi.org/10.5327/Z1519-874X2013000100001

APPENDIX

The following Watershed Description section provides more information on each watershed. Figure A1 presents slow flow hydrographs from the non-calibrated filters and geochemical method for the Ewing subwatershed for 2007 and 2008. Figure A2 shows comparisons between the estimated slow flow components from the non-calibrated filters and geochemical method. Table A1 provides performance measures during the three seasons for 2010 and 2011. Figures A3 and A4 show comparisons of daily fractions of slow flow from the Eckhardt filter and geochemical method for 2010 and 2011 on the upstream and downstream subwatersheds, respectively.

WATERSHED DESCRIPTION

Madawaska Watershed

Located in the Bas-Saint-Laurent region in northeastern Québec, the Madawaska watershed is relatively rugged with steep slopes. Overall, the downstream (Petite Savane) subwatershed has higher average and maximum slopes than the upstream (Couturier) subwatershed. In the northern part of the Madawaska watershed, soils are mainly loam and sandy loam. In the south, soils are mostly loam and silt loam with coarse fragments of shale and slate. In each of the twin subwatersheds, the soils are mostly well drained, but there is about 10% of more imperfectly to poorly drained soils in Couturier. Petite Savane is more forested than Couturier, 55% compared to 46%. On the other hand, the agricultural area is half the size, 20% compared to 41%. According to available data, 29% of the agricultural area in Petite Savane is under perennial crops (hay), while this ratio is 51% in Couturier.

Fourchette Watershed

Both subwatersheds, upstream and downstream, have a hilly relief. Agriculture is practiced over a large part of the upstream subwatershed, while agriculture is limited in the downstream subwatershed. The proportion of the watershed's area under annual crops is 38% in the upstream watershed, compared to 11% in the downstream watershed. The forest cover is more important, covering 38% of the total area of the downstream subwatershed but only 8% of the upstream subwatershed. In the upstream subwatershed, the soils are predominantly argillaceous. The drainage class "very poorly drained" is attributed to 25% of the downstream subwatershed, whereas this class represents only 10% of the upstream subwatershed.

Champlain Watershed

The downstream subwatershed is along the Noire River, while the upstream subwatershed is along the Brûlée River. Both subwatersheds drain into the Champlain River. The agricultural areas of both subwatersheds are located on a relatively hilly landscape. They have an average slope of 2%,

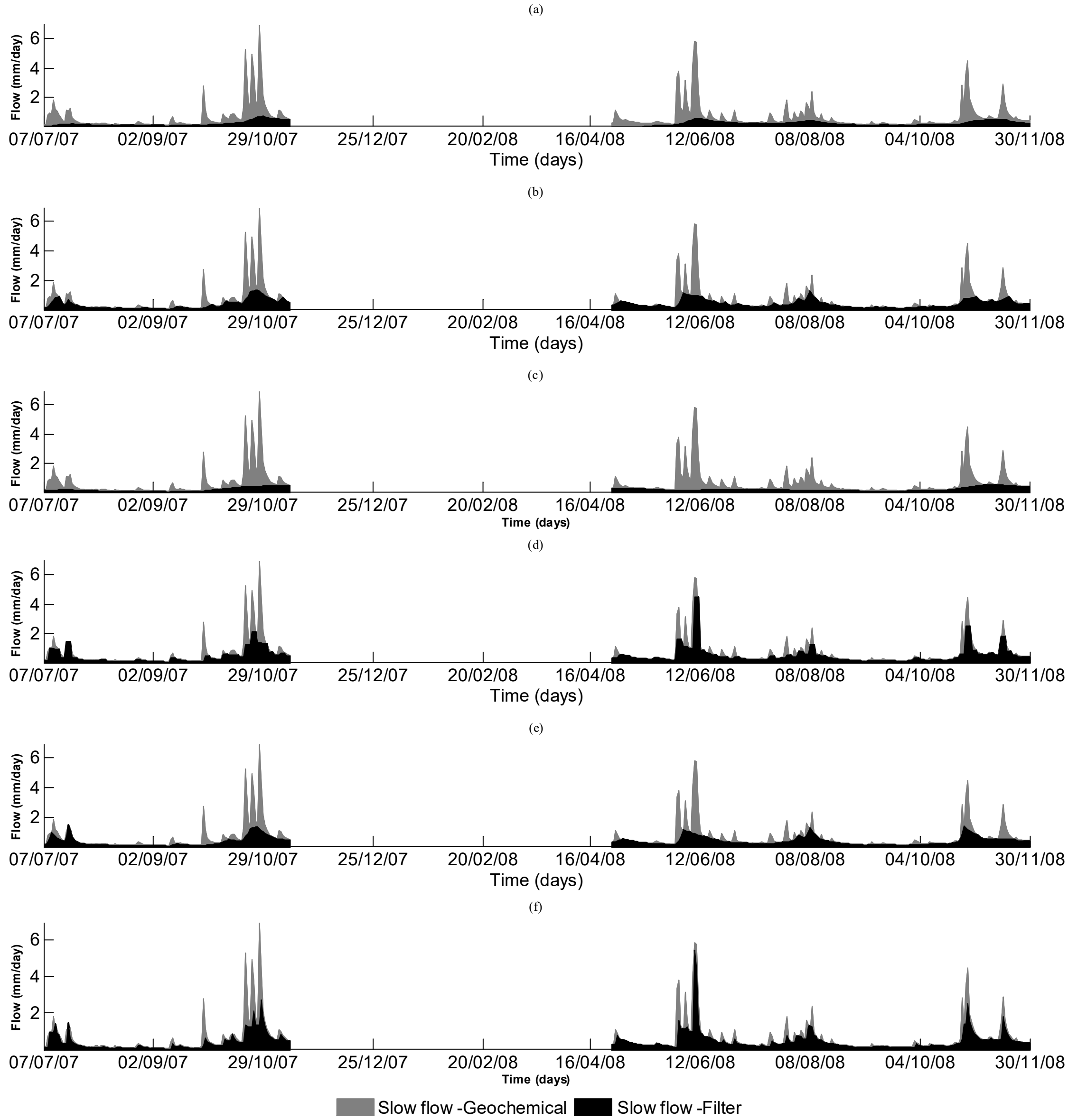

Figure A1. Comparisons of daily slow flows hydrographs from non-calibrated filters and geochemical method for Ewing subwatershed for 2007 and 2008: (a) BFLOW, (b) PART, (c) UKIH, (d) FIXED, (e) LOCMIN, and (f) SLIDE.

but substantially higher maximum slopes are present in the Brûlée subwatershed. Sandy loam soils dominate the Noire subwatershed, while sandy soils occupy one-third of Brûlée. This leads to 60% well drained soils in Noire, compared to 12% in Brûlée, and more than twice as much imperfectly drained soil in Brûlée (as a ratio of the total area of each subwatershed). Noire is a bit more forested than Brûlée, 49% compared to 41%. Agricultural soils cover 47% of Noire and 55% of Brûlée. In Noire, perennial crops cover 13.3% and annual crops cover 11.6%, while in Brûlée, annual crops cover the three-quarters of the agricultural land. The dominant annual crops are corn and soybeans.

Baie Lavallière Watershed

With average slopes of less than 0.7%, the landscape of the subwatersheds is particularly flat. Dominated by coarse soil textures upstream of the watershed and heavier textures downstream, fine loamy sand occupies the largest area in the Bellevue (downstream) subwatershed, while silty clay loam is the dominant texture of the Pot-au-Beurre (upstream) subwatershed. Sandy loams are also present in both subwatersheds. The downstream subwatershed area is 40% forest-covered and 58% under cultivation (with 47% being annual crops). In the upstream subwatershed, forest occupies only 3% of the area, the remaining being cultivated (with 74% of annual crops). Maize dominates, occupying more than 47% and nearly 60% of the cultivated land in the downstream and upstream subwatersheds respectively. The next major crop is soybeans (24% and 12.5%), followed by cereals (6.9% and 2.4%). In both subwatersheds, hayfields occupy less than 10% of the total area (7.9% and 7%) but their proportion of agricultural land is two times higher in the downstream subwatershed (13.5% compared to 7.2%).

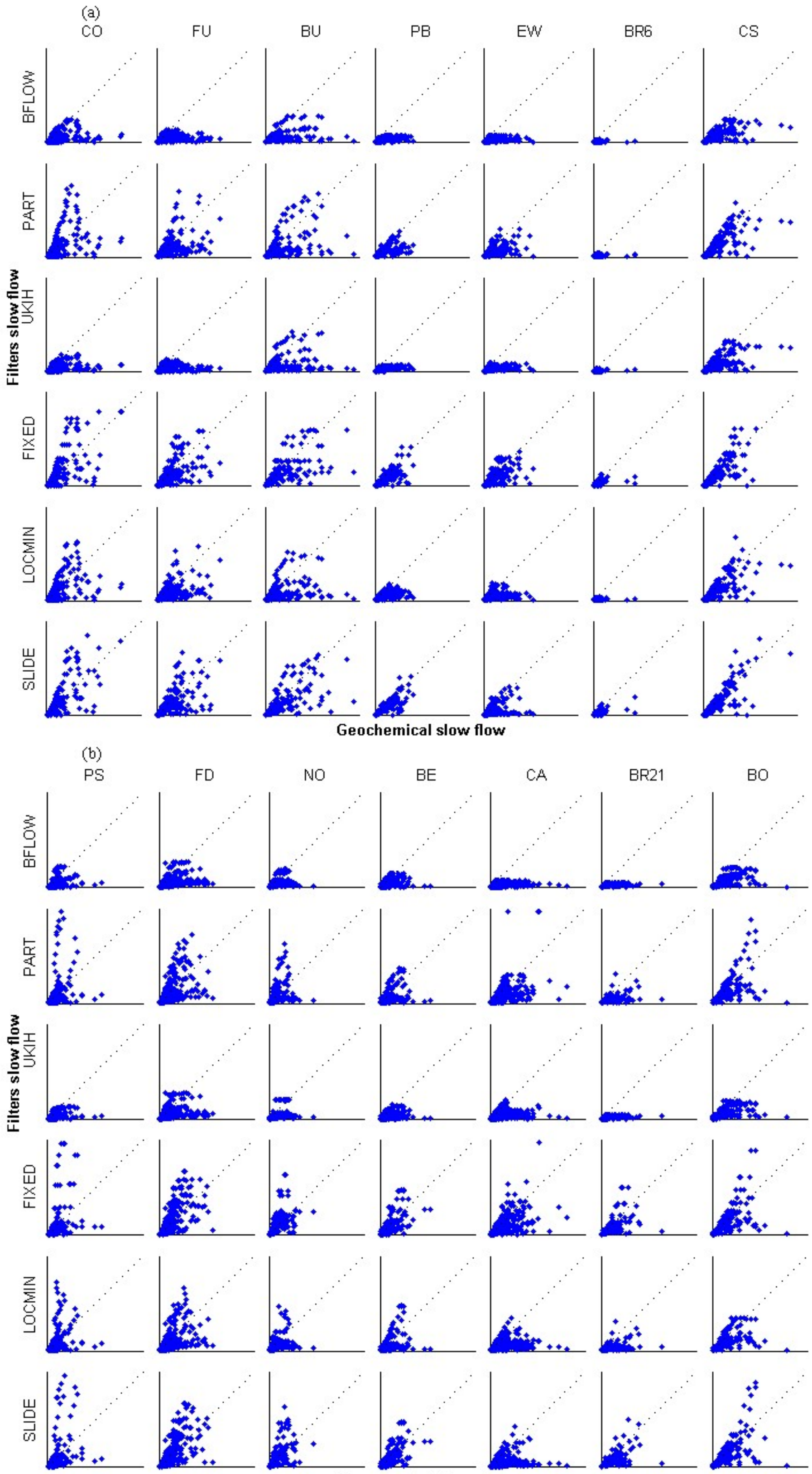

Figure A2. Comparison of daily slow flow estimates (mm d^{-1}) from non-calibrated filters and geochemical method for (a) upstream and (b) downstream subwatersheds. Sites are Couturier (CO), Fourchette upstream (FU), Brûlée (BU), Pot-au-Beurre (PB), Ewing (EW), Branche 6 (BR6), Cass (CS), Petite Savane (PS), Fourchette downstream (FD), Noire (NO), Bellevue (BE), Aux Castors (CA), Branche 21 (BR21), and Brook (BO).

Table A1. Performance statistics (R, NSE, and PBIAS) during spring, summer, and fall seasons in calibration period of 2010 and validation period of 2011 at all sites.

			Spring[b]			Summer[b]			Fall[b]		
Year	Watershed	Subwatershed[a]	R	NSE	PBIAS	R	NSE	PBIAS	R	NSE	PBIAS
2010	Madawaska	CO	0.94	0.68	-0.20*	1.00	0.80	0.35*	1.00	0.80	0.35*
		PS	0.98	0.66	-0.16*	0.99	0.91	0.25*	0.99	0.91	0.25*
	Fourchette	FU	0.97	0.50	-0.05	0.99	0.86	0.36*	0.99	0.86	0.36*
		FD	0.97	0.58	-0.17*	0.99	0.76	0.37*	0.99	0.76	0.37*
	Champlain	BU	0.98	0.88	-0.20*	0.96	0.85	-0.11*	0.96	0.85	-0.11
		NO	0.95	0.52	-0.29*	0.99	0.23	0.46*	0.99	0.23	0.46*
	Baie Lavallière	PB	0.97	0.89	0.03	0.99	0.98	0.04	0.99	0.98	0.04
		BE	0.94	0.69	-0.07	0.99	0.87	0.29*	0.99	0.87	0.29*
	Baie Missisquoi	EW	0.98	0.81	0.01	0.99	0.95	0.18*	0.99	0.95	0.18*
		CA	0.97	0.90	0.09	0.99	0.94	0.21*	0.99	0.94	0.21*
	Esturgeon	BR6	1.00	0.97	-0.01	1.00	0.99	0.06	1.00	0.99	0.06
		BR21	0.97	0.84	0.19*	0.91	0.58	0.00	0.91	0.58	0.00
	Tomifobia	CS	0.98	0.93	0.02	0.98	0.79	-0.02	0.98	0.79	-0.02
		BR	0.99	0.93	0.08	0.97	0.64	-0.02	0.97	0.64	-0.02
2011	Madawaska	CO	0.86	-0.63**	-0.46*	0.99	0.93	0.23*	0.99	0.96	0.10
		PS	0.54	-17.92**	-1.55*	0.97	0.80	-0.06	1.00	0.50	0.11*
	Fourchette	FU	0.87	-0.08**	-0.16*	0.87	0.35	0.06	0.95	0.32	0.01
		FD	0.93	0.55	-0.31*	0.93	0.85	0.16*	0.95	0.87	0.12*
	Champlain	BU	0.91	0.43	-0.37*	0.96	0.72	-0.20*	0.99	0.98	-0.03
		NO	0.72	-2.90**	0.53*	0.96	0.89	-0.02	0.97	0.94	0.04
	Baie Lavallière	PB	0.98	0.85	-0.08	0.93	0.38	-0.12*	0.98	0.91	0.00
		BE	0.95	0.03	-0.34*	0.88	0.22	0.02	0.99	0.90	0.13*
	Baie Missisquoi	EW	0.92	-2.26**	-0.40*	0.92	0.45	-0.18*	0.98	0.64	-0.09
		CA	0.94	-0.33**	-0.26*	0.91	0.58	-0.19*	0.96	0.56	-0.07
	Esturgeon	BR6	0.98	0.15	-0.38*	0.98	0.90	-0.16*	1.00	1.00	0.05
		BR21	0.93	-1.90**	-0.47*	0.95	-2.78**	-0.55*	0.99	0.68	-0.08
	Tomifobia	CS	0.96	-0.14**	-0.36*	0.99	0.89	-0.10*	0.93	-0.93**	-0.25*
		BR	0.94	-1.33**	-0.38*	0.99	0.86	-0.08	0.92	0.53	-0.03

[a] Sites are Couturier (CO), Petite Savane (PS), Fourchette upstream (FU), Fourchette downstream (FD), Brûlée (BU), Noire (NO), Pot-au-Beurre (PB), Bellevue (BE), Ewing (EW), Aux Castors (CA), Branche 6 (BR6), Branche 21 (BR21), Cass (CS), and Brook (BO).

[b] Asterisks indicate (**) negative NSE values and (*) values outside -10% ≤ PBIAS ≤ 10%.

Baie Missisquoi Watershed

The Ewing and Aux Castors subwatersheds have both a landscape that extends across the St. Lawrence lowlands plain and the Appalachian piedmont. The Ewing subwatershed is flat (mean slope < 1%), and surface soils are sandy spodosols to clayey inceptisols overlying poorly drained clay subsoils of marine and lacustrine origin (Michaud et al., 2009b). Agriculture accounts for 98% of the land use and is dominated by annual corn production on sandy soils (47% of fields) and clayey soils (32% of fields) in rotation with soybean and small grains (8% of annual land use), while hayfields with perennial forages occupy 13% of land use in the subwatershed. In the Aux Castors subwatershed, given the low relief and agricultural potential of the soil (mean slope < 1%), crop production is also relatively intensive, with nearly 80% of the area dedicated to annual crops. Clay soils of marine and lacustrine origin (gleysolic) occupy the low-lying areas, whereas calcareous and shaly tills (brunisolic and podzolic) occupy the higher elevations. Three-quarters of the downstream region is cultivated, and cultivated areas of roughly 20%, 30%, and 50%, respectively, are devoted to hayfields, perennial forages, and annual crops (corn and soybean).

Esturgeon Watershed

The topography of the two subwatersheds is generally very flat. The downstream (Branche 21) subwatershed is entirely of mineral soil (heavy and poorly drained clay loam over 98% of the area). In the upstream (Branche 6) subwatershed, 65% of the soils are organic and very poorly drained, while the mineral soils are mainly silty clays (25%). The two experimental subwatersheds are used exclusively for agriculture. There are no forested areas in Branche 21, and forest covers less than 1% of the area in Branche 6. No perennial crops are grown in Branche 6, and they are also poorly represented in Branche 21 (4.3% of the area). In Branche 21, the dominant annual crops are vegetables (49% of the agriculture area) and soybeans (22%), while the dominant annual crops in the Branche 6 are corn (24%), vegetables (15%), and soybeans (12%). In Branche 6, agricultural areas without crop information correspond to 48.6% of the total agricultural area, while in Branche 21, these categories correspond to 12% of the agricultural area.

Tomifobia Watershed

The Cass (upstream) and Brook (downstream) subwatersheds are characterized by quite steep relief with significant slopes. Overall, Brook has lower average and maximum slopes than Cass (average slope of 6.7%). The soil texture in the subwatersheds is mainly loamy (60% of Brook soils and 85% of Cass soils) or sandy loam (39% of Brook soils and 15% of Cass soils). Soil drainage is mostly good, with nearly 35% and 9% of soils naturally showing poor drainage in Brook and Cass, respectively. Forest covers a large part of the two subwatersheds. However, Brook is slightly less wooded than Cass, 46% compared to 53%. The remaining area is mainly agricultural, and perennial crops dominate with proportions of nearly 28% (Brook) and 15% (Cass). The proportion of annual crops (mainly corn) of the overall area is lower, with 8% in Cass and 3% in Brook. Nearly two-

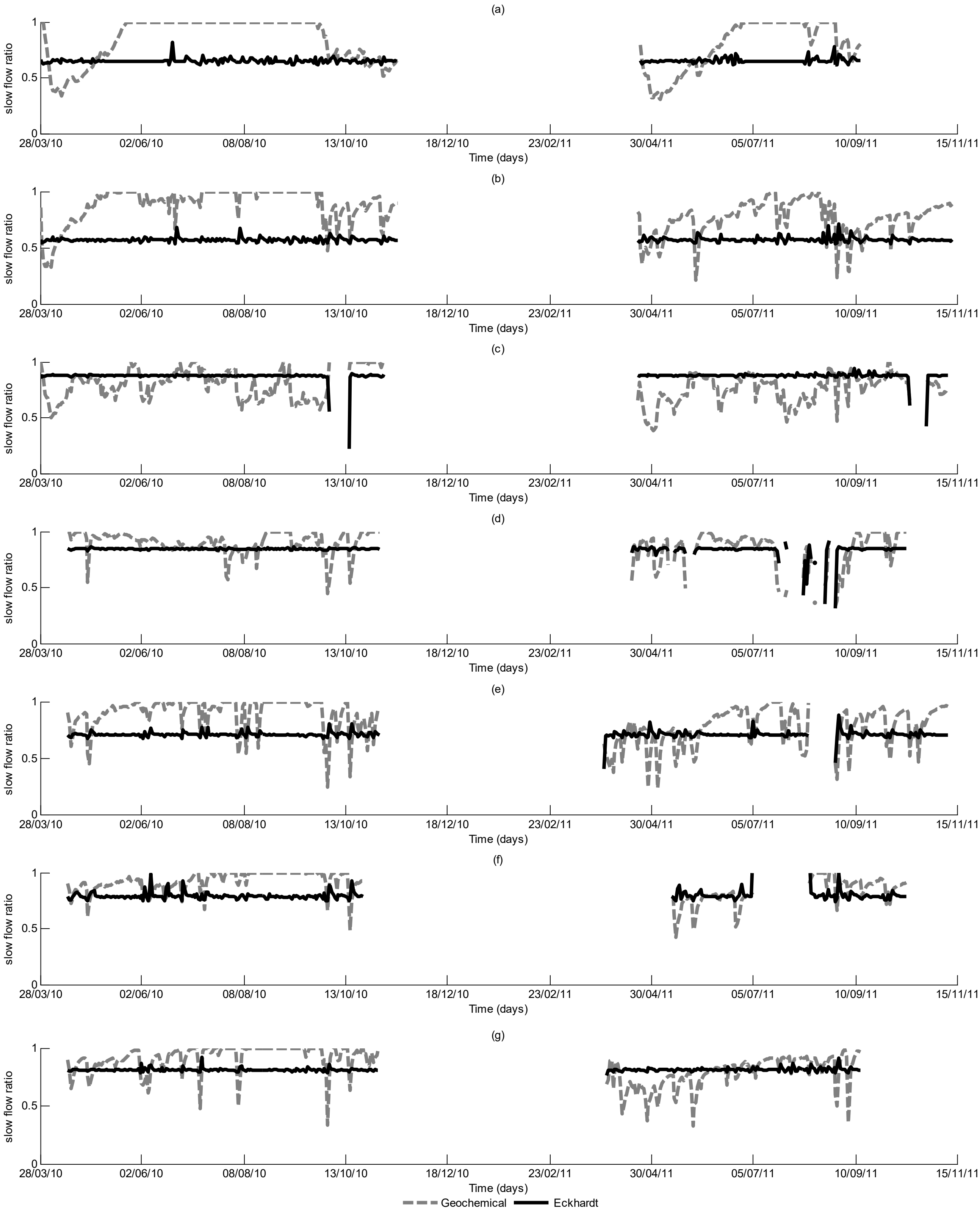

Figure A3. Comparison of daily slow flow fractions from Eckhardt filter and geochemical method over 2010 and 2011 on upstream subwatersheds: (a) Couturier (CO), (b) Fourchette upstream (FU), (c) Brûlée (BU), (d) Pot-au-Beurre (PB), (e) Ewing (EW), (f) Branche 6 (BR6), and (g) Cass (CS). Gaps indicate periods without data.

fifths (37% and 48%) of the agricultural area in the downstream and upstream subwatersheds has no crop information.

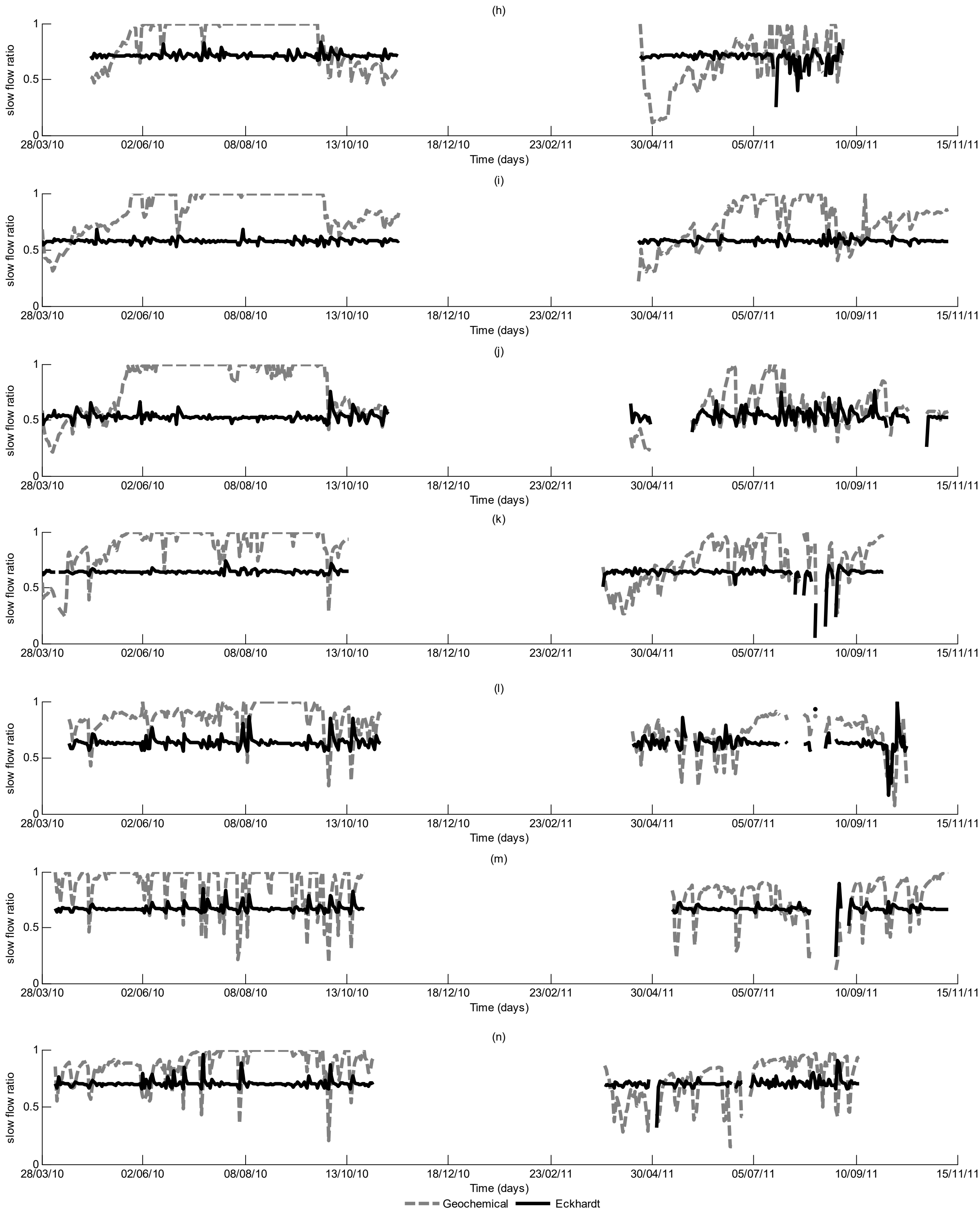

Figure A4. Comparison of daily slow flow fractions from Eckhardt filter and geochemical method over 2010 and 2011 on downstream subwatersheds: (h) Petite Savane (PS), (i) Fourchette downstream (FD), (j) Noire (NO), (k) Bellevue (BE), (l) Aux Castors (CA), (m) Branche 21 (BR21), and (n) Brook (BO). Gaps indicate the periods without data.